

# A Critical Examination of the X-Wind Model for Chondrule and Calcium-rich, Aluminum-rich Inclusion Formation and Radionuclide Production

S. J. Desch

and

M. A. Morris

*School of Earth and Space Exploration, Arizona State University, P. O. Box 871404,  
Tempe, AZ 85287-1404*

and

H. C. Connolly, Jr.

*Kingsborough Community College and the Graduate Center of the City University of New  
York, 2001 Oriental Boulevard, Brooklyn, NY 11235-2398*

*American Museum of Natural History, Central Park West at 79th Street, New York, NY  
10024-5192*

*Lunar and Planetary Laboratory, 1629 E. University Blvd., University of Arizona, Tucson,  
AZ 85721-0092*

and

Alan P. Boss

*Department of Terrestrial Magnetism, Carnegie Institution of Washington, 5241 Broad  
Branch Road NW, Washington, DC 20015-1305*

steve.desch@asu.edu

## ABSTRACT

Meteoritic data, especially regarding chondrules and calcium-rich, aluminum-rich inclusions (CAIs), and isotopic evidence for short-lived radionuclides (SLRs) in the solar nebula, potentially can constrain how planetary systems form. Interpretation of these data demands an astrophysical model, and the “X-wind” model of Shu et al. (1996) and collaborators has been advanced to explain the

origin of chondrules, CAIs and SLRs. It posits that chondrules and CAIs were thermally processed  $< 0.1$  AU from the protostar, then flung by a magnetocentrifugal outflow to the 2-3 AU region to be incorporated into chondrites. Here we critically examine key assumptions and predictions of the X-wind model. We find a number of internal inconsistencies: theory and observation show no solid material exists at 0.1 AU; particles at 0.1 AU cannot escape being accreted into the star; particles at 0.1 AU will collide at speeds high enough to destroy them; thermal sputtering will prevent growth of particles; and launching of particles in magnetocentrifugal outflows is not modeled, and may not be possible. We also identify a number of incorrect predictions of the X-wind model: the oxygen fugacity where CAIs form is orders of magnitude too oxidizing; chondrule cooling rates are orders of magnitude lower than those experienced by barred olivine chondrules; chondrule-matrix complementarity is not predicted; and the SLRs are not produced in their observed proportions. We conclude that the X-wind model is not relevant to chondrule and CAI formation and SLR production. We discuss more plausible models for chondrule and CAI formation and SLR production.

## 1. Introduction

Chondrites, the most primitive known meteorites, are the witnesses to the birth of our solar system. Their parent bodies, which are asteroids, formed some 4.57 billion years ago in the region roughly 2-3 AU from the Sun and have suffered relatively little alteration since then (Wadhwa & Russell 2000). As such, they record conditions (chemistry, pressure, temperature) in the solar nebula. Chondrites are the key to understanding our solar system's birth and, by extension, the processes in protoplanetary disks where planets are forming today.

From a petrological standpoint, most chondrites are analogous to conglomerates, of igneous spheres. Chondrites are remarkable for containing calcium-rich, aluminum-rich inclusions (CAIs), the oldest solids formed in the solar system. The formation of some CAIs has been dated very precisely: Pb-Pb dating of CAIs in the CV3 chondrite NWA 2364 reveals an age  $4568.67 \pm 0.17$  Myr (Bouvier & Wadhwa 2009). The majority of CAIs (all but the Fluffy Type A, and related objects) experienced some degree of melting while floating freely in the solar nebula (Connolly et al. 2006). Type B CAIs, in particular, were heated to high temperatures, followed by cooling over periods of hours (at rates of  $\approx 5$  K hr $^{-1}$ ; Stolper 1982; Stolper & Paque 1986). Also found in abundance within chondrites are sub-millimeter- to millimeter-sized, (mostly ferromagnesian) igneous spheres, called chondrules. Chondrules

formed at most 2 – 3 Myr after CAIs (Amelin et al. 2002; Kita et al. 2005; Russell et al. 2006; Wadhwa et al. 2007; Connelly et al. 2008), as melt droplets that were heated to high temperatures while they were independent, free-floating objects in the early solar nebula, after which they cooled over periods of hours. Chondrules and CAIs together indicate that the components of chondrites were exposed to widespread, energetic, transient heating events.

Unraveling the unusual process that melted chondrules and CAIs is fundamental to understanding the evolution of protoplanetary disks. That the mechanism was intermittent and transient follows directly from the inferred timescales for heating and cooling, which are hours or less. The widespread nature of the mechanism is inferred from the fact that chondrules make up as much as  $\approx 80\%$  of the volume of ordinary chondrites (Grossman 1988). The energies involved are staggering. It is estimated that the current mass of chondrules in the asteroid belt is  $\sim 10^{24}$  g (Levy 1988). The energy required to heat rock 1000 K and then melt it typically exceeds  $3 \times 10^{10}$  erg g $^{-1}$ , so at a minimum  $3 \times 10^{34}$  ergs were required to melt the existing chondrules. For every gram of chondrules in the present-day asteroid belt, though, there were originally perhaps 300 grams, subsequently lost as the asteroid belt was depleted by orbital resonances (Weidenschilling 1977a; Bottke et al. 2005; Weidenschilling et al. 2001). As well, for every gram of rock in the solar nebula there was an associated 200 grams of gas (Lodders 2003). The energy to raise gas 1000 K in temperature exceeds  $3 \times 10^{10}$  erg g $^{-1}$  and thus far outweighs the energy needed to melt chondrules. If chondrules were melted in the solar nebula and were thermally coupled to gas, the energy required to heat the gas, along with all the chondrules inferred to have originally been there, exceeded  $2 \times 10^{39}$  erg. All in all, a remarkable fraction ( $> 1\%$ ) of the gravitational potential energy of the disk mass from 2 to 3 AU was involved in heating the gas during chondrule formation. In doing so, this mysterious mechanism did more than merely melt chondrules and CAIs: it left clues to its nature in the manner in which chondrules and CAIs were melted, cooled and recrystallized. The differences in igneous textures of chondrules and (type B) CAIs, combined with the elemental fractionations within crystals, provide constraints on their thermal histories (Connolly et al. 2006), and therefore provide constraints on the type of transient heating events that melted them.

Since Sorby (1877) first recognized the need to explain the igneous textures of chondrules, numerous mechanisms for melting of chondrules and CAIs have been proposed. Some of the more favored mechanisms include interaction with the early active Sun, through jets (Liffman & Brown 1995, 1996) or magnetic flares (Shu et al. 1996, 1997, 2001); melting by lightning (Pilipp et al. 1998; Desch & Cuzzi 2000); melting by planetesimal impacts (Merrill 1920; Urey & Craig 1953; Urey 1967; Sanders 1996; Lugmair & Shukolyukov 2001); and also passage of solids through nebular shocks (Wood 1963; Hood & Horanyi 1991, 1993; Hewins 1997; Connolly & Love 1998; Hood 1998; Jones et al. 2000; Iida et al. 2001; Desch &

Connolly 2002; Ciesla & Hood 2002; Connolly & Desch 2004; Desch et al. 2005; Connolly et al. 2006; Miura & Nakamoto 2006; Morris & Desch 2010). Of the proposed transient heating mechanisms, the two that have received the most attention and which have been modeled in the most detail have been the nebular shock model and the so-called “X-wind model” of Shu et al. (1996, 1997, 2001). The nebular shock model hypothesizes that chondrule precursors were overtaken by shocks passing through the gas of the solar nebula disk at about the present-day location of the chondrules, the asteroid belt, 2-3 AU from the Sun. The source of these shocks may have been X-ray flares, gravitational instabilities, or bow shocks driven by planetesimals on eccentric orbits (see Desch et al. 2005). Chondrules would be melted by the friction of the supersonic gas streaming past them, thermal exchange with the shocked, compressed gas, as well as by absorption of radiation from other heated chondrules. CAI precursors presumably formed in a hotter portion of the nebula but could have been melted by shocks as well. The X-wind model hypothesizes that solid material was transported to  $< 0.1$  AU from the Sun, formed chondrule and CAI precursors there, were melted, and then were transported back to 2-3 AU.

Additional constraints on processes acting at the birth of the solar system arise from isotopic studies of meteorites, which reveal the presence of short-lived radionuclides (SLRs) in the solar nebula, radioactive isotopes with half-lives of millions or years or less. Although these isotopes have long since decayed, their one-time presence is inferred from excesses in their decay products that correlate with the parent elements. For example, the one-time presence of  $^{26}\text{Al}$ , which decays to  $^{26}\text{Mg}$  with a half-life of 0.71 Myr, is inferred by analyzing several minerals within a given inclusion, and finding excesses in the ratio  $^{26}\text{Mg}/^{24}\text{Mg}$  that correlate with the elemental ratio  $^{27}\text{Al}/^{24}\text{Mg}$ . The excesses are due to  $^{26}\text{Al}$  decay, so the proportionality between the ratios above yields the value of  $^{26}\text{Al}/^{27}\text{Al}$  when the inclusion crystallized (achieved isotopic closure). In this way Lee et al. (1976) inferred an initial abundance  $^{26}\text{Al}/^{27}\text{Al} \approx 5 \times 10^{-5}$  in CAIs from the carbonaceous chondrite Allende. Likewise several more SLRs have been inferred to exist, including such key isotopes as:  $^{60}\text{Fe}$  (Tachibana & Huss 2003), with a half-life  $t_{1/2} = 2.62$  Myr (Rugel et al. 2009);  $^{10}\text{Be}$  (McKeegan et al. 2000), with  $t_{1/2} = 1.5$  Myr; and  $^{36}\text{Cl}$  (Lin et al. 2005), with  $t_{1/2} = 0.36$  Myr.

The origins of these SLRs are debated, as reviewed by Wadhwa et al. (2007). The consensus model, at least for the majority of SLRs, hypothesizes an origin in a nearby core-collapse supernova, either just before or during the formation of the solar system. Supernova material may have been injected into the Sun’s molecular cloud core (Cameron & Truran 1977; Vanhala & Boss 2002), or may have been injected into the Sun’s protoplanetary disk (Chevalier 2000; Ouellette et al. 2005, 2007). Indeed, the abundance of  $^{60}\text{Fe}$  is inconsistent with all models for its origin that do not involve nearby, recent supernovae in the Sun’s

star-forming environment (Wadhwa et al. 2007). On the other hand,  $^{10}\text{Be}$  is not formed significantly in supernovae, and must have an origin distinct from  $^{60}\text{Fe}$ ; this interpretation is supported by the observed decoupling of these two SLRs in meteorites (Marhas et al. 2002). Desch et al. (2004) point out that the abundance of Galactic cosmic rays (GCRs) that are themselves  $^{10}\text{Be}$  nuclei is much higher than the ratio in the solar nebula, and that GCRs trapped in the Sun’s collapsing molecular cloud core will easily lead to the observed meteoritic abundance of  $^{10}\text{Be}$ . We discuss this model in somewhat more detail in §6.3. An alternative model for the origins of the SLRs is that they were created when energetic ( $> \text{MeV nucleon}^{-1}$ ) ions collided with nuclei of rock-forming elements brought  $< 0.1 \text{ AU}$  from the Sun, in the context of the X-wind model (Gounelle et al. 2001). If this were true, a supernova source for the SLRs would not be demanded (except for  $^{60}\text{Fe}$ ). Unraveling the origins of the SLRs has obvious, fundamental implications for where the Sun formed.

The formation of chondrules and CAIs, and the origins of the SLRs, place important constraints on the place of the Sun’s origin, the presence of supernovae in its birth environment, and for processes in its protoplanetary disk. These issues apply more broadly to protostars forming today, and bear on the likelihood of Earth-forming planets. The X-wind model claims to explain chondrule and CAI formation, and the origins of the SLRs, in a unified model. The purpose of this paper is to critically examine the X-wind model. In §2, we first review the meteoritic constraints on the formation of chondrules and CAIs and on the origins of SLRs. We include petrologic constraints arising from the CAI *Inti* found in the *STARDUST* sample return (Zolensky et al. 2006). The X-wind model itself is reviewed in §3. In §4 we discuss internal inconsistencies within the X-wind model, and in §5 we compare its predictions about chondrule and CAI formation and SLR production against the meteoritic constraints. We discuss alternative hypotheses to the X-wind model in §6. In §7 we draw conclusions about the viability of the X-wind model.

## 2. Meteoritic Constraints

Isotopic and petrologic studies of chondrules and CAIs have yielded a wealth of constraints about how these particles formed, and then were melted. Here we review the constraints that all models for the formation of chondrules and CAIs must satisfy. For further descriptions of these constraints, the reader is referred to reviews by Jones et al. (2000), Connolly & Desch (2004), Desch et al. (2005), Connolly et al. (2006), MacPherson (2003), and Ebel (2006). We also review the meteoritic evidence for SLRs and their possible origins. For further details, the reader is referred to Goswami & Vanhala (2000), McKeegan & Davis (2003), Gounelle (2006), and Wadhwa et al. (2007).

## 2.1. Chondrule Formation

The most important constraints on chondrule formation come from experimental constraints on their thermal histories. Chondrules are the result of melting and recrystallization of precursor assemblages, and constraints exist on the initial temperature of chondrule precursors, their peak temperatures and the time spent at these temperatures, as well as the cooling rates from the peak and during crystallization. Here we highlight the main constraints only; the reader is referred to reviews on chondrule thermal histories by Desch & Connolly (2002), Connolly & Desch (2004), Desch et al. (2005), and Hewins et al. (2005), and references therein. The initial temperatures of the chondrule precursors are generally held to be  $< 650$  K, the condensation temperature of S (at least in a solar-composition gas: Lodders 2003), because chondrules contain primary S that was not lost during chondrule formation (Rubin 1999; Jones et al. 2000; Tachibana & Huss 2005; Zanda 2004). Chondrules could not have spent more than a few hours at temperatures higher than  $650 - 1200$  K, depending on pressure (Hewins et al. 1996; Connolly & Love 1998; Rubin 1999; Jones et al. 2000; Lauretta et al. 2001; Tachibana & Huss 2005). The majority of chondrules experienced peak temperatures in the range of  $1770 - 2120$  K for several seconds to minutes (Lofgren & Lanier 1990; Radomsky & Hewins 1990; Hewins & Connolly 1996; Lofgren 1996; Hewins 1997; Connolly et al. 1998; Connolly & Love 1998; Jones et al. 2000; Connolly & Desch 2004; Hewins et al. 2005; Lauretta et al. 2006), although the peak temperatures of barred olivine chondrules may have been as high as  $2200$  K (Connolly et al. 1998). Approximately 15% of chondrules in ordinary chondrites contain relict grains (Jones 1996), whose survival depends on the time spent a chondrule spends at the peak temperature (Lofgren 1996; Connolly & Desch 2004; Hewins et al. 2005). On this basis, chondrules spent only tens of seconds to several minutes at their peak temperatures (Connolly et al. 2006). Likewise, retention of Na and S demands chondrules cooled from their peak temperatures at rates  $\sim 5000 \text{ K hr}^{-1}$ , or several hundred K in a few minutes (Yu et al. 1995; Yu & Hewins 1998). The textures of different chondrule textural types are reproduced experimentally only by certain cooling rates through the crystallization temperature range (roughly  $1400 - 1800$  K for common chondrule compositions). In ordinary chondrites, 84% of chondrules are pophyritic, with many euhedral crystals (Gooding & Keil 1981). These are reproduced by cooling rates  $\approx 5 - 1000 \text{ K hr}^{-1}$  (Jones & Lofgren 1993; Desch & Connolly 2002). Barred olivine textures, with many parallel laths of olivine, make up 4% of ordinary chondrite chondrules (Gooding & Keil 1981), and require cooling rates  $\approx 250 - 5000 \text{ K hr}^{-1}$  (see Desch & Connolly 2002 and references therein). Finally, radial pyroxene textures, with a few crystals radiating from a single nucleation site, account for 8% of ordinary chondrite chondrules (Gooding & Keil 1981). These textures probably require destruction of relict grains and production of a supercooled liquid (Connolly et al. 2006), and can be reproduced by cooling rates in the

range  $5 - 3000 \text{ K hr}^{-1}$  (Lofgren & Russell 1986). Other chondrule textures exist, such as glassy chondrules that presumably cooled even faster than these, but the salient point is that most chondrules were heated to temperatures  $> 1800 - 2000 \text{ K}$  for minutes only, cooling at  $\sim 5000 \text{ K hr}^{-1}$ , then cooled at slower rates  $10^2 - 10^3 \text{ K hr}^{-1}$  through their crystallization temperatures  $1400 - 1800 \text{ K}$ .

Besides these constraints on chondrule thermal histories during the chondrule-forming event, other constraints restrict the timing of chondrule formation. Chondrules contain relict grains, including unmelted fragments of large particles. The texture, chemistry, and oxygen isotopic composition of relict grains indicates that they are fragments of chondrules, formed in previous generations. This signifies that the event that melted chondrules occurred more than once, and that individual chondrules may have experienced multiple heating events (Connolly et al. 2006; Ruzicka et al. 2008; Kita et al. 2008; Connolly et al. 2009). From Al-Mg systematics, most extant chondrules are known to have melted approximately 2 Myr after CAIs formed (Russell et al. 1997; Galy et al. 2000; Tachibana et al. 2003; Bizzarro et al. 2004; Russell et al. 2006). These same data suggest timescales for chondrule formation of several Myr (Huss et al. 2001; Tachibana et al. 2003; Wadhwa et al. 2007; Rudraswami et al. 2008; Hutcheon et al. 2009), with 90% formed between 1.5 and 2.8 Myr after CAIs (Villeneuve et al. 2009). U-Pb systematics confirm these timescales (Amelin et al. 2002; Kita et al. 2005; Russell et al. 2006; Connelly et al. 2008) and, not incidentally, indicate that the Al-Mg system is a valid chronometer and that  $^{26}\text{Al}$  was homogeneously distributed in the solar nebula.

Finally, other constraints restrict the environment in which chondrules formed. Chondrules almost certainly formed in the presence of dust that is to first order the matrix grains in which the chondrules are sited. Matrix in primitive carbonaceous chondrites contains forsterite grains that clearly condensed from the gas and cooled at  $\sim 10^3 \text{ K hr}^{-1}$  below  $1300 \text{ K}$  (Scott & Krot 2005). The similarity in cooling rate suggests that these matrix grains formed in the chondrule-forming events. The cogenetic nature of matrix and chondrules is also strongly supported by the chondrule-matrix chemical complementarity. Relative to a solar composition and to CI chondrites, all chondrules and matrix are depleted in volatiles, even moderate volatiles, and metal-silicate fractionation leads to variable amounts of siderophile elements in chondrites; even the abundances of relatively refractory lithophiles (e.g., Ti, Ca, Al, Si, Mg and Fe) can vary within chondrules and matrix. However, the bulk abundances of refractory lithophiles in many chondrites are closer to solar abundances than the abundances of chondrules or matrix alone, strongly implying that the chondrules and matrix grains *within a given chondrite* formed in the same vicinity within the solar nebula (Palme et al. 1993; Klerner & Palme 2000; Scott & Krot 2005; Ebel et al. 2008; Hezel & Palme 2008). Hezel & Palme (2008) analyzed the Ca/Al ratios in the matrix and chondrules of

Allende and Y-86751, two chondrites almost identical in bulk composition. They found the Ca/Al ratio in the matrix of Allende to be sub-chondritic and the ratio in the matrix to be super-chondritic, with the exact opposite true in Y-86751. Ca and Al would be difficult to redistribute on the parent body, strongly implying that the chondrules and matrix grains within these two chondrites formed from the same batch of material with near-solar composition; the two batches underwent slightly different degrees of fractionation of Ca and Al to form one set of chondrules and matrix in Allende, and another set of chondrules and matrix in Y-86751. The cogenetic nature of chondrules and matrix within a given chondrite means that the chondrite did not form from very different reservoirs of material separated by time and place in the nebula, but in a particular time and place in the solar nebula, from solar-composition material, ostensibly near where chondrites originate today.

The density of chondrules in the chondrule forming region can be estimated as well. Cuzzi & Alexander (2006) have investigated the lack of volatile loss from chondrules, which strongly implies high vapor pressures of volatiles in the chondrule forming region. So that evaporated volatiles remained in the vicinity of chondrules, the volume of gas per chondrule must not exceed  $\sim 0.1 \text{ m}^3$  or, equivalently, the chondrule density was  $> 10 \text{ m}^{-3}$ . So that volatiles not diffuse away from the chondrule-forming region, the chondrule-forming region must have been  $> 10^2 - 10^3 \text{ km}$  in extent. In addition, about 2.4% of chondrules in ordinary chondrites are compound, stuck to another chondrule while semi-molten (Wasson et al. 1995). If chondrules had relative velocities  $< 0.1 \text{ km s}^{-1}$  (to avoid shattering upon impact) and were sufficiently plastic to stick for  $\sim 10^4 - 10^5 \text{ s}$ , then the number density of chondrules ( $\approx 300 \mu\text{m}$  in diameter) must have been  $\approx 0.1 - 1 \text{ m}^{-3}$  (Gooding & Keil 1981), or  $\sim 10 \text{ m}^{-3}$  if the relative velocities were  $\sim 10 \text{ cm s}^{-1}$ , as implied by solar nebula turbulence models (Cuzzi & Hogan 2003). For chondrules with masses  $\approx 3 \times 10^{-4} \text{ g}$ , these number densities imply a mass density of chondrules  $\approx 3 \times 10^{-9} \text{ g cm}^{-3}$ , larger than the nominal gas density,  $\sim 10^{-9} \text{ g cm}^{-3}$  (at 2-3 AU in a disk with 10 times the mass of the minimum mass solar nebula of Weidenschilling 1977a), and implies that the solids-to-gas ratio was locally  $\sim 300$  times greater than the canonical 1%. The enhancement of the solids-to-gas ratio is supported by the inference that the chondrule formation region was also relatively oxidizing. FeO-rich chondrules clearly formed in a gas much more oxidizing than one of a solar composition (Jones et al. 2000; Connolly & Desch 2004; Fedkin et al. 2006). Possibly the elevated oxidation is due to chondrule vapor and/or evaporation of fine dust or water ice also concentrated in the chondrule-forming region (Fedkin et al. 2008; Connolly & Huss 2010). On the other hand, the solids-to-gas ratio may have been highly variable: FeO-poor chondrules apparently formed in a more reducing environment, perhaps one as reducing as a solar-composition gas (Zanda et al. 1994; Jones et al. 2000; Connolly & Desch 2004), although this interpretation is complicated by the possibility of reducing phases in the precursor assemblage such as C, so



that chondrules may not so faithfully record the oxygen fugacity of the chondrule formation region (Connolly et al. 1994; Hewins 1997).

One last, important constraint is the observed correlation between chondrule textures and compound chondrule frequency. In ordinary chondrite chondrules overall, among the population of porphyritic, barred olivine and radial pyroxene textures, 87% are porphyritic, 4% are barred, and 9% are radial (Gooding & Keil 1981). Among compound chondrules in ordinary chondrites, which account for 2.4% of all chondrules, the proportions are 19% porphyritic, 32% barred, and 49% radial (Wasson et al. 1995). Barred olivines and radial pyroxenes are about an order of magnitude more common among compound chondrules than chondrules overall. Despite the rarity of compound chondrules, 24% of barred olivines and 15% of radial pyroxenes are found in the compound chondrule population. Porphyritic textures are consistent with cooling rates  $5 - 1000 \text{ K hr}^{-1}$ , although chemical zoning profiles favor lower cooling rates (Jones & Lofgren 1993; Desch & Connolly 2002), while barred textures are reproduced only with cooling rates  $250 - 3000 \text{ K hr}^{-1}$ . The barred olivine textures that so strongly correlate with compound chondrules appear to require faster cooling rates, by about an order of magnitude (the cooling rates of radial pyroxenes are not well determined, but appear to have been similarly fast). These data strongly imply that chondrule cooling rates were faster where compound chondrules were more likely to form. If the solids-to-gas ratio varied in space, compound chondrules would have formed in regions of higher chondrule density. A positive correlation between chondrule cooling rate and chondrule density is then strongly implied.

## 2.2. CAI Formation

CAIs have long been recognized to be the assemblages of very refractory minerals such as hibonite, anorthite, spinel, perovskite and fassaite and high-temperature reaction products such as gehlenite and melilite that are the first to form from a cooling solar-composition gas (Larimer 1967; Grossman 1972; Ebel & Grossman 2000). These minerals are likely to have condensed out of a solar-composition gas as it cooled below 1800 K (MacPherson 2003; Ebel 2006). The site of this condensation is unknown: it may have occurred near the Sun, or in a transiently heated region farther away. That the gas in the condensation region was of solar composition is supported not just by the mineralogy of CAIs but by constraints on the oxygen fugacity of the CAI formation environment. The valence state of Ti (i.e., the  $\text{Ti}^{4+}/\text{Ti}^{3+}$  ratio) in minerals such as fassaite and rhönite in CAIs, which is sensitive to the  $f\text{O}_2$  during formation, routinely show that CAIs formed in an environment with oxygen fugacity very near that of a solar composition gas, with  $f\text{O}_2 \approx \text{IW} - 6$ , or 6 orders of

magnitude less oxidizing than the Iron-Wustite buffer (Beckett et al. 1986; Krot et al. 2000; Simon et al. 2010; Paque et al. 2010). Recently, the mineral osbornite [(Ti,V)N] has been detected in two CAIs: a CAI within the CB chondrite Isheyevo (Meibom et al. 2007), and the object known as *Inti* collected in the *STARDUST* sample return (Zolensky et al. 2006). Significantly, osbornite can only condense in a gas that is very close in composition and oxidation state to a solar-composition gas, with C/O ratios in the range 0.91 - 0.94 (Ebel 2006; Petaev et al. 2001). It is not possible to condense osbornite in an environment as oxidizing as that associated with chondrule formation, for example.

Most CAIs were melted some time after their minerals condensed and the CAIs formed, but some CAIs (the “Fluffy Type A” CAIs) did not. For one class of melted CAIs (type B), peak temperatures  $\approx 1700$  K are inferred from the crystallization of melilite (Stolper 1982; Stolper & Paque 1986; Beckett et al. 2006). Based on the inhomogeneous concentrations of V, Ti, and Cr within spinel grains, they are constrained to be at these peak temperatures for less than a few tens of hours (Connolly & Burnett 2003). The cooling rates of Type B CAIs have been constrained to  $0.5 - 50 \text{ K hr}^{-1}$  (Paque & Stolper 1983; MacPherson et al. 1984; Simon et al. 1996). Like chondrules, Type B CAIs show such petrographic and geochemical evidence for multiple heating events, including variations in minor element concentrations in spinels and Na content in melilites (Davis & MacPherson, 1996; Beckett et al., 2000, 2006; Connolly & Burnett, 2000; Connolly et al. 2003). According to Beckett et al. (2000), after melting, some CAIs experienced alteration in the nebula before being re-melted. The time of such alteration is still unconstrained, but is clearly less than 1 Myr (Kita et al. 2005, 2010; MacPherson et al. 2010). The overall timescale of CAI production has been constrained from the inferred initial abundance of  $^{26}\text{Al}$  to be  $\sim 10^5$  years (Young et al., 2005; Shahar & Young, 2007; Kita et al., 2010; MacPherson et al., 2010), suggesting that the processing of refractory materials into igneous rocks was relatively rapid and stopped before chondrules were formed (Connolly et al., 2006). Thus, the processing of CAIs within the disk was cyclic over a relatively short time period of at most a few  $\times 10^5$  years, but most likely  $< 10^5$  years (Kita et al., 2010)

Like chondrules, CAIs (at least, those of type B) experienced similar peak temperatures and cooling rates, and multiple melting events. Unlike chondrules, CAIs equilibrated with a reducing gas with near-solar composition. Their formation also occurred earlier in the nebula’s evolution. A reasonable interpretation is that CAIs formed earlier and were melted by a mechanism similar to that that melted chondrules, but that CAIs were melted under different environmental conditions.

### 2.3. Short-Lived Radionuclides

At this time, there are 9 SLRs with half-lives of  $\sim 10^7$  yr or less that are inferred from meteorites to have existed in the early solar system. The list of these SLRs, taken from the review by Wadhwa et al. (2007), is given in Table 1.

The longest lived of these isotopes may have been continuously created over Galactic history and inherited from the Sun’s molecular cloud. Radionuclides are created by a variety of stellar nucleosynthetic processes, including core-collapse supernovae, type Ia supernovae, novae, and outflows from Wolf-Rayet stars and asymptotic-giant-branch (AGB) stars (Wadhwa et al. 2007). These are injected into the interstellar medium at a given rate and subsequently decay. To the extent that the newly created isotopes are injected into the hot phase of the interstellar medium, incorporation of the SLRs into a forming solar system will only occur after the gas cools and condenses into molecular clouds. This process, during which the gas remains isotopically “isolated,” takes considerable time, probably  $\sim 10^8$  yr. Recently Jacobsen (2005) and Huss & Meyer (2009) have included such an isolation time in simple Galactic chemical evolution models, and have used them to predict the abundances of SLRs inherited from the interstellar medium. Whether or not such intermediate-lived SLRs as  $^{53}\text{Mn}$ ,  $^{107}\text{Pd}$  and  $^{182}\text{Hf}$  were inherited is debatable and dependent on input parameters. A substantial fraction of  $^{129}\text{I}$  appears to be mostly inherited from the interstellar medium. In fact, the solar nebula would have far too much of this SLR unless the isolation time exceeds 100 Myr (Huss & Meyer 2009). Inheritance of  $^{53}\text{Mn}$  at meteoritic abundances, however, is not possible with an isolation time longer than  $\sim 50$  Myr, so this isotope was probably not inherited. One robust finding of these studies is that even with a very short isolation time, inheritance from the interstellar medium cannot yield the meteoritic abundances of  $^{41}\text{Ca}$ ,  $^{36}\text{Cl}$ ,  $^{26}\text{Al}$  and  $^{60}\text{Fe}$ . These four SLRs, and probably  $^{53}\text{Mn}$  (and  $^{10}\text{Be}$  for that matter), are diagnostic of a late addition to the solar nebula.

Since the X-wind models were published, strong evidence has arisen for the presence of live  $^{36}\text{Cl}$  ( $t_{1/2} = 0.3$  Myr) in the solar nebula, from Cl-S systematics of sodalite in carbonaceous chondrites, at levels  $^{36}\text{Cl}/^{35}\text{Cl} \sim 4 \times 10^{-6}$  (Lin et al. 2005; Hsu et al. 2006), corroborating earlier hints from Cl-Ar systematics (Murty et al. 1997). As sodalite is thought to be a late-stage product of aqueous alteration, the initial  $^{36}\text{Cl}/^{35}\text{Cl}$  value would have been higher if it were injected by a supernova early in the nebula’s evolution along with other SLRs. An initial value  $^{36}\text{Cl}/^{35}\text{Cl} \sim 10^{-4}$  is usually inferred (Hsu et al. 2006; Wadhwa et al. 2007). More recent analyses of Cl-S systematics in wadalite in the Allende carbonaceous chondrite indicate an even higher ratio,  $^{36}\text{Cl}/^{35}\text{Cl} \approx 1.72 \pm 0.25 \times 10^{-5}$ , implying even higher initial abundances of  $^{36}\text{Cl}$  (Jacobsen et al. 2009). These levels are higher than those thought possible for supernova injection,  $^{36}\text{Cl}/^{35}\text{Cl} \sim 10^{-6}$  (see discussion in Hsu et al. 2006), and

have been interpreted as evidence for a late stage of irradiation within the solar nebula, producing  $^{36}\text{Cl}$  by direct bombardment of target nuclei by energetic ions (Lin et al. 2005; Hsu et al. 2006; Jacobsen et al. 2009). At this point it seems likely that this interpretation is correct, although the time and place in the solar nebula where this irradiation took place are unknown. An irradiation origin of  $^{36}\text{Cl}$  does not necessarily imply an irradiation origin within the X-wind environment.

It is worth noting that Chaussidon et al. (2006) claimed evidence for the one-time presence of  $^7\text{Be}$ , which decays to  $^7\text{Li}$  with a half-life of only 57 days, in a CAI from the carbonaceous chondrite Allende. Li is notoriously mobile and subject to large isotope fractionations by chemical processes. It is very difficult to distinguish radiogenic excesses of  $^7\text{Li}$  for these reasons. Desch & Ouellette (2006) identified several weaknesses of the analysis of Chaussidon et al. (2006). They conclude that while Li indeed appears anomalous in this Allende CAI, perhaps representing an admixture with spallogenic Li, the data are not conclusive whatsoever with any Li being the decay product of  $^7\text{Be}$ .

### 3. Description of the X-wind Model

The X-wind model originally was developed by Shu and collaborators (Shu et al. 1994a,b, 1995; Najita & Shu 1994; Ostriker & Shu 1995), to explain the collimated outflows from protostars. The X-wind model is first and foremost a model of gas dynamics in protostellar systems, and was extended only later to investigate the formation of chondrules and CAIs near the protostar, by Shu et al. (1996), Shu et al. (1997), and Shu et al. (2001), and to investigate nuclear processing of solids, by Lee et al. (1998) and Gounelle et al. (2001). (See also reviews by Shu et al. 2000, Shang et al. 2000.) We note that the model evolved somewhat through the late 1990s; we consider the models of Shu et al. (1996, 2001) for the dynamics and thermal processing of solids, and Gounelle et al. (2001) for the irradiation products, to represent the most recent and most detailed incarnations of the model.

#### 3.1. Dynamics

We begin by summarizing the dynamics of gas and solids in the X-wind model. At its heart, the X-wind is a magnetocentrifugal outflow, as in the classic work of Blandford & Payne (1982). Magnetic field lines are anchored by flux freezing in the protoplanetary disk and forced to co-rotate with it. As they are whipped around by the disk, the inertia of matter tied to the field lines causes the field lines far above and below the disk to bow

outwards. Ionized gas tied to the field lines acts like a bead on a wire: as the field line (wire) is whipped around, the gas (bead) is flung outward. This outflow carries significant angular momentum with it, and gas and entrained solids accrete through the disk.

Gas and solids accrete until they reach the “X point” at a distance  $R_x$  from the protostar. At the X point, the pressure of the stellar magnetic field prevents the inward flow of disk gas and truncates the disk. The value of  $R_x$ , given by Equation 1 of Shu et al. (2001; see also Ghosh & Lamb 1979; Shu et al. 1994a) is easily reproduced under the assumption that the magnetic pressure of the stellar magnetosphere balances the ram pressure of accreting gas in the disk. Outside  $R_x$ , in the disk, gas is tied to open magnetic field lines that cross the disk, and gas is driven outward by a magnetocentrifugal outflow. Inside  $R_x$ , magnetic field lines are tied to the protostar, and gas corotates with the protostar. Formally, the field lines and associated gas do not mix. Shu et al. (1996, 2001) presume that ionization is low enough near the X point to allow matter to diffuse across field lines and cross into the region interior to  $R_x$ , but this stage is not explicitly modeled.

As material crosses the X point, it is heated and expands along field lines. Just farther than the X point, in the disk, where  $T \approx 1500$  K, the scale height of the gas is  $H \sim 2 \times 10^{10}$  cm  $\approx 0.03 R_x$ . If the gas inside the X point is heated so that the scale height increases by a factor of 30, the gas can flow directly onto the protostar, guided by the magnetic field lines in a “funnel flow”. Heating of the gas to  $\sim 10^6$  K is sufficient, and can occur due to heating by X-rays generated by reconnection events interior to the funnel flow. The region interior to the funnel flow, denoted the “reconnection ring”, from  $r \approx 0.75 R_x$  to  $R_x$ , is modeled as having reversed poloidal components across the midplane (Ostriker & Shu 1995), leading to frequent magnetic reconnection events akin to solar flares. Shu et al. (2001) identify this region as a possible source of a component of protostellar X-rays such as those observed by Skinner & Walter (1998). From such observations they infer an electron density  $n_e \approx 3 \times 10^8$  cm $^{-3}$  and temperatures  $T \approx 8 \times 10^6$  K in the reconnection ring, yielding sound speeds  $v_T \sim 400$  km s $^{-1}$ , gas densities  $\approx 5 \times 10^{-16}$  g cm $^{-3}$ , and pressures  $P \sim 10^{-7}$  atm. Indeed, for the X wind model to work, this region needs to be the site of frequent magnetic flares, so that solids in this region are irradiated by energetic ions and undergo nuclear processing.

As gas accretes inward past the X point and joins the funnel flow, Shu et al. (2001) hypothesize that a fraction  $F \sim 0.01$  of the solid material leaves the flow and enters the reconnection ring. This can occur, they say, if solids spiral inward within the disk into the reconnection ring, or if they fail to be lofted by the funnel flow. Once in the reconnection ring, the solid particles orbit at Keplerian speeds through a gas that is corotating with the protostar, and so experience a constant headwind. This causes particles to lose angular momentum and spiral in towards the protostar in a matter of years. They are lost unless the

magnetosphere of the protostar fluctuates, periodically waning so that the disk can encroach on the reconnection ring, sweep up the particles and launch them in a magnetocentrifugal outflow. If they can be launched by the outflow, there is the possibility that the particles can land in the disk, depending on their aerodynamic properties (Shu et al. 1996).

### 3.2. Thermal Processing

Shu et al. (2001) do not explicitly calculate the thermal histories of particles in the X wind. They do not, for example, calculate temperature-dependent cooling rates  $dT/dt$  vs.  $T$ . They do, however, cite two possible mechanisms for thermally processing particles. While in the reconnection ring or the disk, magnetic flares are presumed to heat chondrules and especially CAIs; but CAIs and chondrules are *last* melted by sudden exposure to sunlight as they are lofted away from the disk.

While in the reconnection ring, proto-CAIs are repeatedly exposed to magnetic flares that heat particles, mostly by impacts by energetic ions and absorption of X-rays. Depending on the flare energy luminosity and the area over which it is deposited, CAIs can be mildly heated, destroyed completely in “catastrophic flares”, or heated to the point where just their less refractory minerals evaporate. While in the reconnection ring, it is assumed CAI material repeatedly evaporates and recondenses. An important component of the X-wind model as put forth by Shu et al. (2001) is that heating of proto-CAI material will usually allow evaporation of ferromagnesian silicate material, but leave unevaporated more refractory Ca,Al-rich silicate material. Without this core/mantle segregation, irradiation by energetic ions (discussed below) overproduces  $^{41}\text{Ca}$  with respect to  $^{26}\text{Al}$ . Flares are also presumed to heat chondrules in the transition region between the reconnection ring and the disk. Here the calculation of temperatures is very much intertwined with the structure of the disk and the relative heating rates due to flares and sunlight.

The other mode of heating, and the one causing chondrules and CAIs to melt for the last time before isotopic closure, arises when these particles are lofted by the magnetocentrifugal outflows, above the disk in which they reside. The presumed densities of proto-CAIs in the reconnection ring are such that they will form an optically thick, if geometrically thin, disk. Because this optically thick disk absorbs starlight obliquely, its effective temperature due to heating by starlight,  $T_{\text{disk}}$ , is lower than the particle blackbody temperature  $T_{\text{BB}} = (L_{\star}/16\pi r^2\sigma)^{1/4}$  at that radius (where  $L_{\star}$  is the stellar luminosity and  $\sigma$  the Stefan-Boltzmann constant). Particles start within the disk at temperatures  $\approx T_{\text{disk}}$ , but as they are lofted their temperatures rise to  $T_{\text{BB}}$  as they are exposed to starlight. Actually, they reach slightly higher  $T$  because they are exposed to the radiation emitted by the disk, as well; Shu et al. (1996,

2001) approximate this particle temperature, the highest temperatures particles will reach, as  $T_{\text{peak}} \approx (T_{\text{disk}}^4/2 + T_{\text{BB}}^4)^{1/4}$ . For the parameters adopted by Shu et al. (1996, 2001) for the “embedded” phase (in which  $\dot{M} \approx 2 \times 10^{-6} M_{\odot} \text{yr}^{-1}$ ), we find  $T_{\text{BB}} \approx 1700 \text{ K}$ ,  $T_{\text{disk}} \approx 1160 \text{ K}$ , and  $T_{\text{peak}} \approx 1750 \text{ K}$  (approximately what Shu et al. 1996 find). Thus, Shu et al. (1996) state that launching either a CAI or chondrule in an outflow can raise its temperature from  $< 1200 \text{ K}$  to  $1800 \text{ K}$  or more, within a span of “a few hours.” This timescale is set by the dynamics of the particle, which must travel roughly a scale height in the vertical direction. As the heated CAIs or chondrules are flung to great distances, the absorption of starlight lessens, and they cool. It is straightforward to demonstrate that the cooling rates in this scenario are necessarily

$$\frac{dT}{dt} \approx -\frac{1}{2} \frac{v_r}{r} T_{\text{BB}}(r). \quad (1)$$

For the trajectories depicted in Figure 2 of Shu et al. (1996),  $v_r \approx 50 \text{ km s}^{-1}$  at  $r \approx 0.1 \text{ AU}$  where particles will cool through their crystallization temperatures. This means that all particles—CAIs and chondrules—necessarily cool from their peak temperatures at the same rate, about  $10 \text{ K hr}^{-1}$ .

### 3.3. Radionuclide Production

A final, major component of the X-wind model is the production of SLRs in CAIs. The reconnection ring is the site of frequent magnetic reconnection events. If these act like solar flares, they could accelerate hydrogen and helium ions to energies in excess of  $1 \text{ MeV/nucleon}$ . Gounelle et al. (2001) hypothesize that flares akin to solar “gradual” flares and “impulsive” flares will take place in the ring, and that ions are accelerated with the same efficiency, relative to the X-ray luminosity, as in the solar atmosphere. The flux today of energetic ( $E > 10 \text{ MeV nucleon}^{-1}$ ) ions at  $1 \text{ AU}$  today is roughly  $100 \text{ cm}^{-2} \text{ s}^{-1}$ , yielding an energetic particle luminosity  $L_p \sim 0.09 L_x$  (Lee et al. 1998). Because T Tauri stars have X-ray luminosities, presumably from flares, roughly five orders of magnitude greater (Feigelson & Montmerle 1999; Feigelson et al. 2007; Getman et al. 2008 and references therein), the fluence of such particles over, say, 20 years, if concentrated into the reconnection ring with area  $\sim 10^{24} \text{ cm}^2$ , would reach  $\sim 2 \times 10^{19} \text{ cm}^{-2}$ . Flares more akin to gradual flares would accelerate mostly protons and alpha particles and lead to an energetic particle spectrum  $\propto E^{-2}$ , while flares akin to impulsive flares would accelerate a comparable number of  ${}^3\text{He}$  ions, and lead to an energetic particle spectrum  $\propto E^{-4}$ . Proto-CAI material in the reconnection ring is constantly bombarded by these energetic ions, which can initiate nuclear reactions in the rocky material, creating new isotopes.

Gounelle et al. (2001) simultaneously model the production of several SLRs within the

context of the X-wind model, attempting to match their initial abundances as inferred from meteorites. They model the production of 4 isotopes in particular:  $^{10}\text{Be}$  ( $t_{1/2} = 1.5$  Myr),  $^{26}\text{Al}$  ( $t_{1/2} = 0.7$  Myr),  $^{41}\text{Ca}$  ( $t_{1/2} = 0.1$  Myr), and  $^{53}\text{Mn}$  ( $t_{1/2} = 3.7$  Myr). They also model production of the very long-lived isotopes  $^{138}\text{La}$  ( $t_{1/2} > 10^{12}$  yr) and  $^{50}\text{V}$  ( $t_{1/2} \sim 10^{11}$  yr), on the grounds that these are not produced in abundance by stellar nucleosynthesis. Of course, these isotopes are so long-lived that they are not diagnostic of irradiation in the solar nebula; they could have been produced by spallation in molecular clouds over Galactic history, for example. We therefore focus on the discussion in Gounelle et al. (2001) of  $^{10}\text{Be}$ ,  $^{26}\text{Al}$ ,  $^{41}\text{Ca}$  and  $^{53}\text{Mn}$ . These are produced overwhelmingly (but not exclusively) by nuclear reactions of H and He ions with O, Mg and Al, Ca, and Fe nuclei, respectively.

Among the first findings of Gounelle et al. (2001) is that uniform irradiation of the average composition of proto-CAIs will result in orders of magnitude more  $^{41}\text{Ca}$ , relative to  $^{26}\text{Al}$ , than is observed in CAIs. They found no way to reconcile the production rates of these two isotopes by irradiation, unless two conditions were met: Ca (the primary target for  $^{41}\text{Ca}$ ) were sequestered in a core; and the thickness of a Ca-free mantle surrounding the core were sufficiently thick to stop energetic ions. Gounelle et al. (2001) assume that repeated evaporations of proto-CAIs preferentially leave behind a residue of Ca,Al-rich refractory cores, onto which ferromagnesian silicates can condense. Under these assumptions, Gounelle et al. (2001) found core sizes for which the meteoritic abundances of the 4 radionuclides above were reproduced, to within factors of a few.

## 4. Internal Inconsistencies of the X-wind Model

### 4.1. Are Jets Launched by X Winds?

Protostellar jets are virtually ubiquitous among protostars. Moreover, jets are associated with strong magnetic fields and are apparently collimated by magnetic hoop stresses (Ray et al. 2007). These observations strongly support models of protostellar outflows as magnetocentrifugally launched. They are also taken at times as support for the X-wind model in particular (Shu et al. 2000), but it must be emphasized that jets could be taken as evidence for the X-wind only if they can be shown to be launched from inside about 0.1 AU. An ongoing debate in the astronomical community is whether protostellar jets are launched from locations  $\sim 0.1$  AU from the protostar, as in the X-wind, or from  $\sim 1$  AU, as advocated by proponents of “disk wind” models (Wardle & Königl 1993; Königl & Pudritz 2000; Pudritz et al. 2007). To be blunt: just because one observes a protostellar jet and magnetocentrifugal outflow from a disk does *not* mean that jets are launched from 0.1 AU, let alone that solids in that disk are transported from a few AU, to 0.1 AU, back out to a



few AU.

In fact, the astronomical evidence at this time does not support the X-wind model, and instead favors disk wind models. Observations of radial velocities across jets reveal their angular momenta and the launch point of the protostellar jets (Bacciotti et al. 2002; Anderson et al. 2003; Coffey et al. 2004, 2007). These observations are technically challenging and were only possible when the *Hubble Space Telescope* / Space Telescope Imaging Spectrograph (*HST*-STIS) was operational. Not all observations were successful; in some cases jet rotation was not observed. In other cases rotation was observed, but in the opposite sense of the disk’s presumed rotation, complicating the interpretation (Cabrit et al. 2006; Pety et al. 2006; Coffey et al. 2007; Lee et al. 2006, 2007). Prograde jet rotation was observed in some protostellar systems, though; in those systems jets appear to be launched from much farther in the disk than the X point. Coffey et al. (2004) observed jet rotation in RW Aur and LkH $\alpha$ 321, and more detailed observations were carried out by Coffey et al. (2007). In DG Tau, a high-velocity component appears launched from about 0.2 - 0.5 AU and a low-velocity component from as far as 1.9 AU; in TH 28, the jet seems launched from about 1.0 - 3.9 AU; and in CW Tau, from 0.5-0.6 AU (Coffey et al. 2007). These authors admit they have not resolved the innermost jet and cannot exclude a contribution from an X-wind; but Woitas et al. (2005) estimate that the jets carry at least 60-70% of the angular momentum to be extracted from the disk. Clearly the disk winds dominate in these systems. As yet, there is no direct evidence from observations of jet rotation that outflows are launched by an X-wind rather than disk winds.

#### 4.2. Solids at the X point?

Besides the question of whether outflows are launched from inside 0.1 AU at all, a second major obstacle for the X-wind model is that neither the model itself nor astronomical observations support the existence of solids at the X point. The theoretical grounds for a lack of solids at the X point are simple. In calculating the temperature of disk material, Shu et al. (1996, 2001) neglected the heating of the disk due to its own accretion, focusing only on the passive heating of the disk by starlight. Specifically, they set

$$\sigma T_{\text{disk}}^4 = \frac{L_{\star}}{4\pi^2 R_{\star}^2} \left[ \arcsin\left(\frac{R_{\star}}{r}\right) - \left(\frac{R_{\star}}{r}\right) \left(1 - \frac{R_{\star}^2}{r^2}\right)^{1/2} \right], \quad (2)$$

which for parameters they consider typical of the embedded phase ( $L_{\star} = 4.4 L_{\odot}$ ,  $r = R_{\text{x}} = 4R_{\star} = 12R_{\odot}$ ) yields  $T_{\text{disk}} \approx 1160$  K. For parameters they consider typical of the revealed phase ( $L_{\star} = 2.5 L_{\odot}$ ,  $r = R_{\text{x}} = 5.3R_{\star} = 16R_{\odot}$ ),  $T_{\text{disk}} \approx 820$  K. But an additional term must

be added to the right side of Equation 2 to account for energy released by disk accretion. Setting

$$\sigma T_{\text{acc}}^4 = \frac{3}{8\pi} \dot{M} \Omega^2, \quad (3)$$

we can better estimate the effective temperature of the disk (approximately the temperature at optical depths  $\approx 1$  into the disk’s surface) as

$$\sigma T_{\text{eff}}^4 = \sigma T_{\text{disk}}^4 + \sigma T_{\text{acc}}^4, \quad (4)$$

(Hubeny 1990). Using  $\Omega \approx 8 \times 10^{-6} \text{ s}^{-1}$  at the X point and assuming a mass accretion rate of  $2 \times 10^{-6} M_{\odot} \text{ yr}^{-1}$  for the embedded phase, one derives  $T_{\text{acc}} = 2030 \text{ K}$  and a temperature  $T_{\text{eff}} \approx 2090 \text{ K}$ , sufficient to evaporate all solids. Even if one uses the lower mass accretion rate  $\dot{M} \approx 1 \times 10^{-7} M_{\odot} \text{ yr}^{-1}$ , appropriate for the revealed stage,  $T_{\text{acc}} = 960 \text{ K}$  and  $T_{\text{eff}} \approx 1070 \text{ K}$ . The effective temperature is approximately the temperature at optical depths  $\approx 1$  into the disk’s surface.

These high temperatures are exacerbated by the fact that  $T_{\text{eff}}$  is a lower limit to the temperatures experienced by particles. The effective temperature is approximately the temperature of the disk at 1 optical depth into the disk. Because accretional heating must be transported out of the disk by a radiative flux, temperatures inside the disk, at optical depths  $\gg 1$  (using the Rosseland mean opacity) will exceed  $T_{\text{eff}}$ , by a factor  $\approx (3\tau/8)^{1/4}$  (Hubeny 1990). For even moderate optical depths (e.g.,  $\tau = 10$ ), temperatures will rise above 1500 K, even for the lower mass accretion rates of the revealed stage. Considering optical depths  $\ll 1$ , temperatures will also exceed  $T_{\text{eff}}$ , because the particles will be exposed to starlight directly. An isolated particle at a distance  $r$  from the protostar will achieve a blackbody temperature

$$T_{\text{BB}} = \left( \frac{L_{\star}}{16\pi\sigma r^2} \right)^{1/4}. \quad (5)$$

For particles at the X point,  $T_{\text{BB}} \approx 1700 \text{ K}$  during the embedded stage, and  $\approx 1280 \text{ K}$  during the revealed stage. In addition to the direct starlight, particles in the uppermost layers of the disk will also absorb radiation from the disk as well, achieving temperatures well approximated by

$$T^4 \approx \frac{1}{2} T_{\text{eff}}^4 + T_{\text{BB}}^4 \quad (6)$$

(Shu et al. 1996). Even for the revealed stage, this temperature is 1360 K. Finally, if the dust particles in the uppermost layers are submicron in size, they will absorb optical radiation but will be unable to radiate in the infrared effectively, and they will achieve even higher temperatures still. Chiang & Goldreich (1997) have explained the excess near-infrared emission in spectral energy distributions (SEDs) of protostellar disks by accounting for this “superheated” dust layer. Even during the revealed stage, then, particles in the

uppermost layers of the disk at the X point will achieve temperatures in excess of 1360 K. The significance of the dust temperatures  $> 1360$  K is that silicates are not stable against evaporation such high temperatures (at least in the disk environment discussed here, mixed in a solar ratio with  $\text{H}_2$  gas). Above 1400 K, for example, dust grains will evaporate in only hours (Morris & Desch 2010). Thus, temperatures are simply too high to have a dusty disk approach all the way to the X point, even during the “revealed” stage, when mass accretion rates are  $\leq 10^{-7} M_{\odot} \text{yr}^{-1}$ . A calculation of the innermost radius where dust can stably reside is complicated by the “wall-like” structure of the disk there, and the poorly known thermodynamic properties of dust materials, but has been considered by Kama et al. (2009), who show that typically the inner edge where solids can exist is typically several  $\times 0.1$  AU from a protostar.

Astronomical observations confirm the absence of solids at the X point. Eisner et al. (2005) have determined the inner edges of dust emission in the protoplanetary disks surrounding 4 Sun-like protostars, through a combination of NIR interferometry and SED fitting. Through measurements of other stellar properties, they also determined the locations of the corotation radius and the predicted locations of the X point. They find that typically the corotation radius and magnetospheric truncation radius are both  $< 0.1$  AU and agree within the uncertainties, but that the inner edge of the dust disk also typically lies beyond either of these radii, at about  $0.1 - 0.3$  AU. This is true even for V2508 Oph, the protostar with the least discrepancy (among the 4 sampled) between the X point and the inner edge of the dust disk. It is also a protostar with parameters that closely match those adopted by Shu et al. (1996, 2001) for a protostellar system in the revealed stage:  $M_{\star} = 0.9 M_{\odot}$ ,  $\dot{M} = 2.3 \times 10^{-7} M_{\odot} \text{yr}^{-1}$ , and an age  $\approx 0.6$  Myr. Eisner et al. (2005) attribute the existence of an inner edge to the dust disk to sublimation of dust at that radius, consistent with their observation that the maximum temperature associated with dust emission is in the range 1000 - 2000 K ( $\approx 1500$  K for V2508 Oph, albeit with considerable uncertainty). Eisner et al. (2005) also note that in systems with higher mass accretion rates, the X point (by construction) is pushed inward, and they observed the inner edge of the dust disk to move outward. This finding is also consistent with dust sublimation being the cause of the inner edge of the disk. Based on the theoretical arguments above, and the observations of Eisner et al. (2005), solid particles are not expected to exist at the X point in disks with mass accretion rates  $> 10^{-7} M_{\odot} \text{yr}^{-1}$ . Altogether, by neglecting accretional heating, Shu et al. (1996, 2001) appear to have underestimated the temperatures of solids, and predicted them to exist where they should not be and, indeed, are not observed to be.

### 4.3. Decoupling from the Funnel Flow?

In order for the X-wind model to be a valid description of CAI or chondrule formation, these objects must adhere to a specific dynamical history. Specifically, Shu et al. (2001) assumed that a fraction  $F \sim 0.01$  of all solid material decouples from the funnel flow and enters the reconnection ring. It is presumed to do so because it is bound in solid particles that experience a gravitational force greater than the drag force exerted on them by the funnel flow. We argue above that all material should evaporate at the X point, but assuming solids to exist, their dynamical histories will depend critically on their sizes. Clearly protoplanetary disks contain sub-micron and micron-sized grains, as evidenced by silicate emission features at  $10 \mu\text{m}$  (e.g., Sargent et al. 2009). Shu et al. (1996, 2001) specifically identify these micron-sized solid particles with matrix grains in chondrites. Importantly, within the context of the X-wind model, there are no other particles in chondrites that can be identified as pre-existing in the protoplanetary disk, because chondrules and CAIs form in the X-wind environment, and not in the disk. Chondrites also contain large aggregations of smaller particles that are unmelted, only lightly sintered and lithified, termed agglomeratic chondrules; but these are rare, making up only 2% of the volume of ordinary chondrites (Dodd & van Schmus 1971; Weisberg & Prinz 1996). We discuss these below, but for now assert that if chondrules do not form in the disk, then for practical purposes the only solid material entering the funnel flow would be micron-sized grains.

Because solid particles in the disk are so small, they are almost certain to couple strongly to the gas as it enters the funnel flow. According to Weidenschilling (1977b), small particles with aerodynamic stopping times much less than the dynamical time will basically move with the gas, but with a small relative velocity  $(\Delta g)t_{\text{stop}}$ , where

$$t_{\text{stop}} = \frac{\rho_s a}{\rho_g v_T} \quad (7)$$

is the aerodynamic stopping time [in the Epstein drag limit where particles are smaller than the mean free path of gas molecules, appropriate for micron-sized particles in gas with density  $< 10^{-4} \text{ g cm}^{-3}$ , or chondrules in gas with density  $< 10^{-7} \text{ g cm}^{-3}$ ], where  $\rho_s$  and  $a$  are the particle density and radius,  $\rho_g$  and  $v_T$  are the gas density and thermal velocity, and  $\Delta g$  is the difference between the accelerations felt by the gas and solids.

In the context of the disk proper,  $\Delta g$  is the extra acceleration the gas feels because of pressure support,

$$\Delta g = \frac{1}{\rho_g} \frac{\partial P_g}{\partial r}, \quad (8)$$

where  $P_g$  is the gas density. Assuming  $T \approx 1500 \text{ K}$  just outside the X point,  $\Delta g \sim v_T^2/r \sim 0.1 \text{ cm s}^{-2}$  (neglecting terms of order unity). The disk scale height is  $H \sim 2 \times 10^{10} \text{ cm}$ , and

assuming a minimum mass solar nebula (Weidenschilling et al. 1977a), we estimate a disk density  $\Sigma \sim 10^5 \text{ g cm}^{-2}$  at the X point, yielding a gas density  $\rho_g \sim 10^{-6} \text{ g cm}^{-3}$ . For a particle with radius  $a = 1 \mu\text{m}$  and internal density  $\rho_s = 3 \text{ g cm}^{-3}$ , the aerodynamic stopping time is  $t_{\text{stop}} \sim 10^{-3} \text{ s}$ . The relative velocity between gas and dust, within the disk, is therefore  $\sim 10^{-4} \text{ cm s}^{-1}$ . This relative velocity is negligible, and gas and dust can be considered perfectly coupled.

In the context of the transition between the disk and the funnel flow,  $\Delta g$  is given by the acceleration the gas experiences. Shu et al. (1996, 2001) do not explicitly model this stage, but we can estimate the acceleration as follows. The gas starts essentially from rest at the X point, but by the time it participates in the funnel flow it could be moving as much as the thermal velocity in the reconnection ring,  $V \sim 400 \text{ km s}^{-1}$ . The distance over which this occurs is perhaps  $d \sim 0.1 R_x \sim 10^{11} \text{ cm}$ . Thus  $\Delta g \sim V^2/d \sim 10^4 \text{ cm s}^{-2}$  (about 10 g’s). As for the stopping time, we derive a lower limit to the gas density in the funnel flow by assuming that it carries a total mass flux  $\dot{M}_*$  onto the star. The funnel flow arises from an area  $A$ , and is composed of gas moving at a velocity  $V$ , with density  $\rho_g = \dot{M}_*/(AV)$ . The lower limit to the density is found by setting  $A$  and  $V$  as large as they can be, and using the smallest value of  $\dot{M}_*$ . The absolute largest  $A$  can be is  $4\pi R_x^2 \sim 8 \times 10^{24} \text{ cm}^2$ , but the size of the reconnection ring,  $\sim 1 \times 10^{24} \text{ cm}^2$ , is probably still an overestimate to the true value of  $A$ . We take the thermal velocity of the gas (after heating to  $10^7 \text{ K}$ ),  $v_T \sim 400 \text{ km s}^{-1}$ , to represent the maximum velocity of the gas. Thus  $\rho_g > 10^{-13} \text{ g cm}^{-3}$  in the funnel flow, and  $t_{\text{stop}} < 10^2 \text{ s}$ . Micron-sized particles (or their aerodynamic equivalents) therefore reach relative velocities with respect to the gas no more than  $\sim (\Delta g)t_{\text{stop}} < 10 \text{ km s}^{-1}$ . This velocity sounds significant [indeed, it would probably lead to evaporation of the dust grains by frictional drag cf. Harker & Desch (2002)] until it is remembered that it is only 2% of the total velocity: both gas and solid particles will move on nearly identical funnel-flow trajectories. Over the roughly 1 hour ( $= d/V$ ) the gas takes to accelerate from the disk to the funnel flow, particles will be displaced only about  $2 \times 10^9 \text{ cm} = 0.002 R_x$ , a negligible amount. Put another way, if gas is funneled onto one spot on the protostar, taking  $\sim 10 \text{ hr}$  to reach it, dust grains will arrive 10 minutes later, at a spot about 1% of the protostar’s radius away.

Shu et al. (2001) argue that solid particles can “fall out” of the funnel flow if the gravitational force on them exceeds the drag force lifting them. This requires

$$\frac{4\pi}{3}\rho_s a^3 \Omega^2 z > \pi a^2 \rho_g (C_D/2) V_g^2, \quad (9)$$

where  $z$  is the height above the midplane. Taking  $z \sim H \sim 2 \times 10^{10} \text{ cm}$  (the scale height of the disk), and  $C_D = (2/3)(\pi k T_p / \bar{m})^{1/2} / V_g$  (Gombosi et al. 1986), the condition to fall out

of the flow becomes a lower limit to the particle size:

$$a > a_{\text{crit}} = \frac{1}{4\rho_s\Omega^2 z} \left( \frac{\pi k T_p}{\bar{m}} \right)^{1/2} \frac{\dot{M}_\star}{A}, \quad (10)$$

where the same relationship between mass accretion rate and gas density in the funnel flow as above was used. Taking  $T_p = 1500$  K,  $\bar{m} = 0.6 m_H$ , a mass accretion rate  $\sim 10^{-7} M_\odot \text{ yr}^{-1}$  and area  $\sim 10^{24} \text{ cm}^2$ , the critical particle diameter to fall out of the funnel flow is  $\sim 4$  mm, and is much larger for higher mass accretion rates.

The conclusion to be reached from all this is that solid material accreting inward, from the disk, through the X point, will remain coupled to the gas as it participates in a funnel flow, unless the solid material in the funnel flow is aerodynamically equivalent to *compact* spheres, several millimeters in diameter. Such particles cannot be chondrules and CAIs, since these are presumed not to form in the disk in the X-wind model, and matrix grains are clearly too small to dynamically decouple from the gas. Agglomeratic chondrules are larger than matrix grains, with diameters 0.3 – 1 mm typically, but that is still too small to decouple from the funnel flow. This is true even if they were compact objects in the nebula gas, but models of coagulation predict that such aggregates would be fractal in shape (Dominik & Tielens 1997). It is quite possible these objects compacted only during accretion onto the parent body; if so, they would have behaved aerodynamically like the smallest particles of which they are composed, i.e., like micron-sized grains (Dominik & Tielens 1997), making it even less likely that they could have decoupled from the funnel flow. Finally, the fact that agglomeratic chondrules make up only 2% of the volume of ordinary chondrites (Weisberg & Prinz 1996), while chondrules make up 85% (Gooding & Keil 1981) is difficult to reconcile with the idea that chondrules and CAIs formed, with low efficiency, from such agglomerations. Thus, there is no significant (i.e., at the  $\sim 1\%$  level) component of solid material in the disk that can be expected to decouple from the funnel flow. The assumption that a fraction  $F \sim 0.01$  of all solid material would leave the funnel flow and enter the reconnection ring, an assumption Shu et al. (2001) themselves term “*ad hoc*,” appears invalid. Even if solid material existed at the X point, the fraction that would fall out of the funnel flow would be  $\ll 0.01$ .

#### 4.4. Survival and Growth in the Reconnection Ring?

The arguments above suggest that solids would not decouple from the funnel flow. Assuming anyway that solid material can enter the reconnection ring, we examine the dynamics of particles there, and also their growth and survival. Growth of solid material in the reconnection ring is much dependent on the dynamics of particles, because the relative velocities  $w$  between particles will determine the sticking coefficient  $S$ , the probability that the two

particles will stick rather than bounce off or even destroy each other. Shu et al. (2001) note (after their Equation 31) that  $w$  is implicitly assumed to be small enough that “molten rocks stick rather than splatter on colliding”. The upper limit on  $w$  obviously will depend on particle composition and whether it is molten or solid, but a typical upper limit adopted in the literature on compound chondrules, which are molten as they collide, is  $\sim 0.1 \text{ km s}^{-1}$  (e.g., Gooding & Keil 1981; Ciesla & Hood 2004). Dominik & Tielens (1997) calculate that solid particles will on average shatter if they collide at velocities  $> 0.01 \text{ km s}^{-1}$ . In any plausible scenario, however, falling out of the funnel flow would impart vertical velocities to particles comparable to the Keplerian velocities,  $\sim 10^2 \text{ km s}^{-1}$ , essentially putting particles on orbits with different inclinations. Necessarily, the relative velocities between particles will also be comparable to these Keplerian velocities. The gas drag forces acting on the particles in the reconnection ring are completely inadequate to slow the incoming particles before they collide with and destroy particles already in the reconnection ring (the surface density of gas,  $\sim 10^{-5} \text{ g cm}^{-2}$ , will not stop even micron-sized particles in less than dozens of disk crossings, while the optical depth of particles in the reconnection ring is large enough to ensure an impact with every crossing). Thus the actual relative velocities of colliding particles in the reconnection ring would exceed the shattering limit, by orders of magnitude.

Put another way, so that particles in the reconnection ring do not collide and shatter, they must exist in a very thin disk with low dispersion of relative velocities,  $w_z$ . Defining, as Shu et al. (2001) do,  $w_z \sim \alpha w$ , where  $\alpha \sim 0.3$ , then the scale height of the disk of proto-CAIs would have to be  $H_r \sim w_z/\Omega \sim 3 \times 10^8 \text{ cm} \sim 10^{-2}$  times the scale height of the disk proper, in order for most particles not shatter each other on impact. As particles would overwhelmingly exit the funnel flow at much greater heights above the disk, it is inevitable that they would not collect in the reconnection ring, but rather shatter upon impact there.

We calculate the effect of all of these particles falling out of the funnel flow as follows. Assuming the mass flux in the funnel flow is  $\dot{M} \sim 10^{-7} M_\odot \text{ yr}^{-1}$ , and a fraction  $\sim 10^{-2}$  of that is in the form of solids, of which a portion  $\sim 10^{-2}$  decouples from the funnel flow, then the flux of particles into the reconnection ring is  $\sim 10^{-11} M_\odot \text{ yr}^{-1}$ , or  $\sim 2 \times 10^{22} \text{ g yr}^{-1}$ . Spreading out this flux of particles over the area of the reconnection ring  $\sim 10^{24} \text{ cm}^2$ , we estimate a solid particle flux  $\sim 2 \times 10^{-2} \text{ g cm}^{-2} \text{ yr}^{-1}$ . A growing CAI has a radius  $> 100 \mu\text{m}$  and a cross section  $\sim 3 \times 10^{-4} \text{ cm}^2$ , and so intercepts a mass  $> 6 \times 10^{-6} \text{ g yr}^{-1}$  from solid particles falling out of the funnel flow, or  $\approx 2 \times 10^{-4} \text{ g}$  over 30 years. This mass exceeds by a large factor the mass of the growing CAI itself, so it is easy to see that a growing CAI will collide with its own mass over its residence time in the disk, at speeds far exceeding tens of km/s. This alone will prevent particles from growing in this environment.

Supposing anyway that the relative velocities are slow enough so that particles don't

shatter, it still is not clear that the sticking coefficient will be sufficient to allow growth. Shu et al. (2001) suggest that  $S$  might be low unless particles are molten, immediately following heating by a flare. Since flares have a limited extent and duty cycle, Shu et al. (2001) adopt an effective sticking coefficient  $S \sim 8 \times 10^{-4} (2\pi)^{1/2} \alpha$ , or  $S < 10^{-3}$ , as typical. To assume a higher value for  $S$ , particles would have to somehow stick even while completely solid. Shu et al. (2001) calculate the mass flux onto a particle as

$$4\pi a^2 \rho_s \frac{da}{dt} \approx + \frac{3}{4(2\pi)^{1/2}} (\Sigma_r \Omega) \frac{S}{\alpha}, \quad (11)$$

where  $\Sigma_r$  is the assumed surface density of rock in the reconnection ring. (NB: This appears to overestimate the growth rate by a factor  $3(\pi/8)^{1/2} \sim 2$ .) The important points about this formula are that the time rate of change of particle radius is independent of radius, and that the growth rate is proportional to the surface density of rocky material, which only reaches a maximum value  $\sim \Sigma_r \sim 1.6 \text{ g cm}^{-2}$  about 30 years after the last “flushing” of the reconnection ring. It is smaller at earlier times (see Figure 4 of Shu et al. 2001). For their preferred value of  $S$ , the maximum growth rate (at 30 yr) is seen from Figure 4 of Shu et al. (2001) to reach  $da/dt \sim +0.03 \text{ cm yr}^{-1}$  at late times (10 years or later). From 1-2 years, the growth rates are much smaller,  $< 3 \times 10^{-4} \text{ cm yr}^{-1}$ .

These growth rates are to be compared to the rate at which hydrogen ions in the plasma thermally sputter the proto-CAIs, an effect neglected by Shu et al. (2001). The density of hydrogen ions arises straightforwardly from the density of hydrogen gas Shu et al. (2001) assume is trapped on field lines crossing the reconnection ring,  $\sim 5 \times 10^{-16} \text{ g cm}^{-3}$ . Jones (2004) gives a simple formula for the sputtering rate in a hot plasma:  $da/dt \sim -(n_H/10^{10} \text{ cm}^{-3}) \text{ yr}^{-1}$ . For  $n_H \sim 3 \times 10^8 \text{ cm}^{-3}$ , this means even a large 1 cm CAI will be completely sputtered in only 30 yr. A more detailed discussion can be found in Draine & Salpeter (1979), who calculate that in a  $T \sim 10^7 \text{ K}$  plasma, each impacting H ion yields roughly 0.02 atoms liberated from an impacted silicate (and 0.2 atoms per impact of He ions). Given the flux of H atoms  $n_H v_T/4 \sim 3 \times 10^{15} \text{ cm}^{-2} \text{ s}^{-1}$  in the ring, it is straightforward to show that particles, again, shrink at a rate  $da/dt \sim -0.03 \text{ cm yr}^{-1}$ . This is competitive with the fastest growth rates of the largest particles at about 30 years, implying that for the sticking coefficient assumed by Shu et al. (2001), particles do not grow faster than they are sputtered. The sputtering rate is independent of particle size, and acts even when particles are small. Thus, about 1 year after material has been flushed out of the reconnection ring, when the largest particles are about 70 microns in radius (according to Shu et al. 2001), thermal sputtering acts about 100 times faster than growth by vapor deposition. Particles at this stage could only grow if the effective (time-averaged) sticking coefficient were  $> 0.1$ , which is implausibly high. Neglect of thermal sputtering by Shu et al. (2001) is a serious oversight; inclusion of this effect shows that particles will not survive, nor grow, in the reconnection ring.



#### 4.5. Retrieval in a Magnetocentrifugal Outflow?

Above we have argued that large particles cannot grow in the reconnection ring, because they are likely to be sputtered before they grow, or are likely to collide fast enough to shatter each other. Assuming that particles do grow, and do have low relative velocities, then in principle they could be launched in magnetocentrifugal outflows when the protostellar magnetic cycle ebbs and the disk encroaches on the reconnection ring; but in practice it is not clear that particles can be launched. Gas orbiting the protostar is launched in a magnetocentrifugal outflow when it is tied to magnetic field lines inclined from vertical by a critical amount ( $60^\circ$ ). Ionized gas is tied to magnetic field lines (because of flux freezing) like beads on a wire; when these wires are inclined to the vertical and spun around an axis, the beads tied to the wire are flung outward. Because of symmetry, magnetic field lines are exactly vertical when they penetrate the midplane of a protoplanetary disk; gas at the midplane will not be flung outward. Wardle & Königl (1993) have examined the vertical structure of accretion disks from which gas is being magnetocentrifugally launched. They find that such outflows are launched only from heights  $z$  above the midplane in excess of 2 gas pressure heights  $H$ .

In order to be launched in a magnetocentrifugal outflow, large particles must be located at least  $2H$  above the midplane; if they are not, they will be tied to gas that is not moving upward and is not being flung out along field lines. For parameters typical of the inner edge of the disk ( $T = 1500$  K sound speed  $2.3 \text{ km s}^{-1}$ ,  $\Omega = 1 \times 10^{-5} \text{ s}^{-1}$ ), the pressure scale height is  $H \sim C/\Omega = 2 \times 10^{10} \text{ cm}$ , and particles must reach heights  $z > 4 \times 10^{10} \text{ cm}$  above the midplane to be launched. The actual vertical distribution of particles as the disk encroaches on them is much smaller, though, on the order of  $w_z/\Omega$ . As  $w_z < 0.03 \text{ km s}^{-1}$  by necessity (or else proto-CAIs would shatter on impact and never grow), their vertical distribution is limited to  $z < 3 \times 10^8 \text{ cm}$ , at least initially. Without some intervening mechanism to vertically spread them, these CAIs will never be launched. Shu et al. (2001) do not identify such a mechanism.

The most plausible mechanism for lofting large particles above the midplane is turbulence, perhaps driven by a magnetorotational instability (MRI) acting at the X point, as Shu et al. (2001) suggest acts to transfer gas across the X point. Several opposing constraints must be satisfied for this to occur. According to the X wind model, the magnetic diffusivity of the gas must be sufficiently high that mass can diffuse off of field lines threading the disk, and onto field lines tied to the star; but the diffusivity can not be so high that it suppresses the MRI generating the turbulence. It is not clear these conditions can both be met: a magnetic diffusivity  $> 0.3 H^2 \Omega \sim 2 \times 10^{15} \text{ cm}^2 \text{ s}^{-1}$  at the X point will suppress the MRI (e.g., Desch 2004); on the other hand, for matter to radially diffuse a distance  $\sim 0.1 R_x$  in 1 yr

requires a comparable diffusivity  $> 2 \times 10^{14} \text{ cm}^2 \text{ s}^{-1}$ . At any rate, detailed modeling of the X point is required before the MRI can be invoked as a source of turbulence, let alone yield the exact turbulence needed to loft CAI-sized particles. In the absence of such a mechanism, the proto-CAIs in the reconnection ring will retain whatever vertical distribution they exhibited there, and they will not be launched.

A lack of detailed modeling also hinders judgment of the last element of launching in the magnetocentrifugal outflow, the final trajectories taken by launched CAIs. Examples of calculated trajectories are presented in Shu et al. (1996) but the calculations on which they are based have not appeared in the refereed literature. One conclusion about these trajectories that is probably robust is that the trajectories taken by specific particles are *highly* sensitive to their aerodynamic properties. Shu et al. (1996) define a parameter  $\alpha$ , inversely proportional to the product a particle’s density and radius. Particles with identical  $\alpha$  will follow identical trajectories, but particles with slightly differing  $\alpha$  will follow greatly varying trajectories. A factor of 2 variation in particle size is the difference between falling back onto the disk at 0.2 AU, or leaving the solar system altogether. Given this sensitivity, it is not clear that many particles would be of the right size to be launched on trajectories that deposit them in the 2-3 AU region.

## 5. X-Wind Model Predictions and Meteoritic Constraints

The X-wind model, as reviewed above, has many internal inconsistencies. It also makes predictions about the formation of chondrules and CAIs that are inconsistent with their petrology and other meteoritic constraints. Formation of SLRs in their meteoritic abundances also faces difficulties in the context of the X-wind model. These inconsistencies are discussed in this section.

### 5.1. Chondrule Formation

The X-wind model is inconsistent with the thermal histories of chondrule formation, constraints on which were discussed in §2. The typical disk temperatures just outside the X point, where chondrules form in the X-wind model, are typically  $> 1160 \text{ K}$ , far higher than the temperatures ( $\approx 650 \text{ K}$ ) require to condense primary sulfur. The cooling rates of chondrules in the X-wind model are  $\sim 10 \text{ K hr}^{-1}$  for all particles. These cooling rates match those required to produce porphyritic chondrule textures as they pass through their crystallization temperatures; but they are not consistent with the cooling rates of barred

olivine chondrules,  $250 - 3000 \text{ K hr}^{-1}$ . They also are not consistent with the much more rapid cooling rates above the liquidus, needed to retain volatiles such as S and Na. Finally, the correlation between chondrule cooling rate and the compound chondrule frequency, which is a robust prediction of the nebular shock model (Desch & Connolly 2002; Ciesla & Hood 2002), is unexplained by the X-wind model.

Some aspects of the chondrule formation environment in the X-wind model are consistent with constraints, others not. The chondrule formation environment is not explicitly modeled within the X-wind model, but we can estimate the gas density. Adopting a minimum-mass solar nebula profile (Weidenschilling 1977a), we infer a gas density  $\approx 2 \times 10^{-6}$  at 0.05 AU, or higher if the disk mass exceeds the minimum-mass solar nebula mass. Assuming a typical solids/gas density ratio  $5 \times 10^{-3}$  and a typical chondrule mass  $\approx 3 \times 10^{-4} \text{ g}$ , we infer a number density of chondrules  $\approx 30 \text{ m}^{-3}$ . This is slightly higher but not inconsistent with the density of chondrules based on compound chondrule frequency and volatile retention. One prediction by the X-wind model about the chondrule formation environment is robust, though: chondrules were heated near 0.1 AU and launched to the 2-3 AU region, where they joined cold dust that had never been heated. This is inconsistent with the presence of matrix dust that was indeed heated to high temperatures, even condensed, in the chondrite-forming region (Scott & Krot 2005). Micron-sized matrix grains launched by the X-wind are predicted to not fall back on the disk, so it is difficult to explain the presence of such grains. Moreover, matrix grains and chondrules within a given chondrite are chemically complementary (at least in their refractory lithophiles), meaning that chondrules and matrix grains are derived from the same batch of solar-composition material.

Finally, the X-wind, model predicts that chondrules and CAIs are formed contemporaneously, and offers no explanation for the observed time difference  $\sim 2 \text{ Myr}$  between CAI and chondrule formation.

## 5.2. CAI Formation

One of the successes of the X-wind model was its prediction that comets would contain CAIs (Shu et al. 1996), like the inclusion *Inti* retrieved by the *STARDUST* mission from comet Wild 2 (Zolensky et al. 2006), although other physical models also predict outward transport of CAIs in the disk (Desch 2007; Ciesla 2007). The X-wind model is inconsistent with many other aspects of CAI formation. It is a robust prediction of the X-wind model that CAIs should evaporate and recondense in a very oxidizing environment. According to Shu et al. (2001), the density of hydrogen gas in the reconnection ring is  $\mathcal{C}^{-1} \times (2 \times 10^{-16}) \text{ g cm}^{-3}$ , where  $\mathcal{C}$  is a dimensionless quantity near unity (see discussion before their equation 12).

Alternatively, they estimate the electron density in this region to be  $n_e \approx 3 \times 10^8 \text{ cm}^{-3}$ . For an ionized hydrogen gas, this yields a density  $5 \times 10^{-16} \text{ g cm}^{-3}$ , which is the value we adopt. In the X-wind model, proto-CAIs grow by condensation following large flares that evaporate much of the solid material. Following an event that evaporates all of the ferromagnesian mantle material from proto-CAIs, Shu et al. (2001) estimate (their §5.1) a surface density  $\sim 1.6 \text{ g cm}^{-2}$  of rocky material (presumably FeO, MgO and SiO<sub>2</sub>) in the gas phase. Initially this material is confined to the volume occupied by the thin disk of proto-CAIs, but it will thermally expand. If it is allowed to expand along field lines more than  $\sim 10^{12} \text{ cm}$  above the reconnection ring, the gas will be lost to the protostar; Shu et al. (2001) assert that the gas will cool before that time. At any rate, the very lowest density the rock vapor can have corresponds to the maximum vertical distribution of about  $10^{12} \text{ cm}$ , which yields a density of rock vapor  $\sim (1.6 \text{ g cm}^{-2}) / (2 \times 10^{12} \text{ cm}) \sim 1 \times 10^{-12} \text{ g cm}^{-3}$ . That is, the mass density of heavy elements is 2000 times the density of hydrogen. This is to be compared to the ratio in a solar-composition gas,  $\sim 0.015$ . Expressed as an oxygen fugacity, it is seen that CAIs materials condense out of a gas that is over 5 orders of magnitude more oxidizing than a solar-composition gas, i.e., with  $f\text{O}_2 \approx \text{IW} - 1$ . The high oxygen fugacity of the gas in the reconnection ring during the times when gas is condensing onto proto-CAIs is completely inconsistent with the barometers of oxygen fugacity such as Ti valence states in fassaite and rhönite, which imply a near solar-composition gas (Krot et al. 2000). It is also inconsistent with the condensation of osbornite in some CAIs, especially in the object known as *Inti* in the *STARDUST* sample return (Meibom et al. 2007); the osbornite also must have condensed in a solar composition gas (Ebel & Grossman 2000). Indeed, the presence of N in the reconnection ring in the first place may itself be problematic, as it should be quickly swept up in the funnel flow.

### 5.3. Radionuclide Production

The X-wind model was developed to explain the abundances of the SLRs <sup>41</sup>Ca, <sup>26</sup>Al, <sup>53</sup>Mn and <sup>10</sup>Be together, but in fact the model has difficulty matching the meteoritic abundances of these SLRs. In the X-wind model, production of <sup>26</sup>Al without overproducing <sup>41</sup>Ca requires that ferromagnesian silicate mantles surround CAI-like refractory cores, and that the two components form immiscible melts during heating. This absolute need arises because in their model <sup>41</sup>Ca is produced by spallation of <sup>40</sup>Ca, whereas <sup>26</sup>Al is produced from spallation of Mg. Without sequestration of Ca in a core, beneath a mantle  $> 1 \text{ mm}$  thick to shield solar energetic particles, <sup>41</sup>Ca is consistently overproduced in the X-wind model, relative to <sup>26</sup>Al. Shu et al. (2001) argue that Ca and Al should be sequestered in a core using theoretical arguments, but experiments consistently show that Ca,Al-rich silicates have a

lower melting point than ferromagnesian silicates and do not form immiscible melts as Shu et al. (2001) describe, instead being well mixed (Simon et al. 2002).

Significantly, both radionuclides are underproduced relative to  $^{10}\text{Be}$  in the X-wind model. This is because the dominant target nucleus,  $^{16}\text{O}$ , is distributed throughout the CAI, and because the reaction proceeds most rapidly due to higher energy ( $\sim 50$  MeV nucleon $^{-1}$ ) solar energetic particles that can penetrate the CAI. Gounelle et al. (2001) were able to marginally co-produce  $^{26}\text{Al}$  and  $^{10}\text{Be}$  using a theoretically derived rate for the reaction  $^3\text{He}(^{24}\text{Mg}, p)^{26}\text{Al}$ . In fact, this reaction rate has been experimentally measured and found to be 3 times smaller than Gounelle et al. (2001) had assumed (Fitoussi et al. 2004), meaning that  $^{10}\text{Be}$  is overproduced by at least a factor of 3 relative to  $^{26}\text{Al}$  in CAIs in the X-wind model. Recent modeling of radionuclide production in the X-wind environment confirms the overabundance of  $^{10}\text{Be}$  relative to  $^{26}\text{Al}$  (Sahijpal & Gupta 2009). The discrepancy is worsened if, in fact, the majority of  $^{10}\text{Be}$  comes from trapped GCRs, as advocated by Desch et al. (2004).

The X-wind model is not capable of explaining the presence of  $^{60}\text{Fe}$  in the early solar system. The neutron-rich isotope  $^{60}\text{Fe}$  is underproduced relative to other radionuclides (e.g.,  $^{26}\text{Al}$ ) by orders of magnitude (Leya et al. 2003; Gounelle 2006). In order to explain the abundance of  $^{60}\text{Fe}$  in the solar nebula, a separate, nucleosynthetic source is required, probably a single nearby supernova (or a small number of nearby supernovae), which could have injected many other SLRs at the same time.

The presence of  $^{36}\text{Cl}$  also does not appear to be explained by the X-wind model. Its presence in the solar nebula has been interpreted as evidence for a late stage of irradiation within the solar nebula, producing  $^{36}\text{Cl}$  by direct bombardment of target nuclei by energetic ions (Lin et al. 2005; Hsu et al. 2006; Jacobsen et al. 2009). The X-wind model provides a natural environment for irradiation to take place, but production of  $^{36}\text{Cl}$  requires irradiation of the target nuclei S, Cl, Ar, and K. The 50% condensation temperatures of all of these elements exceed 1000 K (Lodders 2003), so at the X-point none of these elements will condense. If any of these elements are carried into the reconnection ring, they will quickly evaporate and join the funnel flow and be accreted onto the star. Significantly, if  $^{36}\text{Cl}$  were created in the reconnection ring, it would fail to recondense following the evaporation of CAI material. The presence of live  $^{36}\text{Cl}$  in meteoritic inclusions perhaps implies irradiation, but only in a relatively cold environment ( $< 1000$  K), far cooler than the X-wind model predicts. The fact that the  $^{36}\text{Cl}$  occurs in late-stage alteration products like sodalite also argues against production at the same time CAI were forming.

Within the context of the X-wind model, the SLRs  $^{10}\text{Be}$ ,  $^{41}\text{Ca}$ ,  $^{26}\text{Al}$  and  $^{53}\text{Mn}$  are coproduced in their observed proportions only after making assumptions about the behavior

of CAI melts and the cross section of the  $^{16}\text{O}(p, x)^{10}\text{Be}$  reaction that are not justified. In particular,  $^{10}\text{Be}$  is likely to be overproduced significantly relative to other SLRs in the X-wind environment. The X-wind model also provides no explanation for  $^{60}\text{Fe}$  and  $^{36}\text{Cl}$  in the early solar system, and these SLRs must have a separate origin, perhaps a nearby supernova or irradiation in colder regions of the disk. It is likely that these other sources would contribute to the inventories of other SLRs as well. This is not to rule out contributions from the X-wind, but to point out that the X-wind model must be seen as one model among many alternatives. We now consider the ability of alternative models to explain chondrule and CAI formation, and the origins of the SLRs.

## 6. Alternatives to the X Wind

The X-wind model attempted to connect three distinct problems in meteoritics to a single astrophysical model, to advance the field toward “an astrophysical theory of chondrites”. The problems of chondrule formation, CAI formation, and the origins of the SLRs are not wholly unconnected. On the other hand, extensive petrological and cosmochemical measurements had already led, and have continued to lead, the meteoritics community to develop detailed theories for each of these problems. We summarize these here, to provide the astrophysics community with a current review of these fields, and to provide a comparison for the X wind model, so that its successes and failures can be put into a proper perspective.

### 6.1. Chondrule Formation

At this time, the leading model for chondrule formation is passage through nebular shock waves, in the protoplanetary disk. The model was first proposed by Wood (1963) and subsequently developed by Hood & Horanyi (1991, 1993), Connolly & Love (1998), Hood (1998), Iida et al. (2001), Desch & Connolly (2002), Ciesla & Hood (2002), Miura & Nakamoto (2006), and Morris & Desch (2010). Reviews of chondrule formation and the shock model can be found in Jones et al. (2000), Connolly & Desch (2004), Desch et al. (2005), Hewins et al. (2005), and Connolly et al. (2006). Two leading candidates for the source of the shocks are gravitational instabilities that drive spiral shocks through the disk, or bow shocks around planetesimals on eccentric orbits. Gravitational instabilities would naturally produce large shocks at high speeds compatible with the shock models, if the disk can be shown to be unstable (Boss & Durisen 2005; Boley & Durisen 2008). Because instability requires a cold, massive disk, it may be delayed until mass piles up in the disk and the disk cools; a delay of 2 Myr is not unreasonable. Planetesimal bow shocks should be ubiquitous

if planetesimals form early (by some process that does not rely on chondrule formation) and Jupiter can pump up the eccentricities of these bodies (Hood et al. 2009). Formation of a massive Jupiter might take 2 Myr, so a delay between CAI and chondrule formation is again not unreasonable. The two shock models and their relative merits are discussed further by Desch et al. (2005). In either model of chondrule formation by shocks, chondrule precursors are melted in the disk, at about 2-3 AU, in the presence of dust, thereby complying with the constraints of chondrule-matrix complementarity and the presence of condensate grains discussed above. Turbulence in the disk is capable of generating regions of varying chondrule density (Cuzzi et al. 2001, 2008; Teitler et al. 2009), exceeding  $10^2$  on lengthscales  $\sim 10^4$  km (Hogan & Cuzzi 2007; Cuzzi et al. 2008). The shock wave is presumed to advance through the disk, and individual chondrules would be melted in microenvironments varying in chondrule density and oxidation state.

The models of Desch & Connolly (2002) and Ciesla & Hood (2002), as well as Morris & Desch (2010), are in general agreement and calculate similar thermal histories for chondrules. A typical case is depicted in Figure 1, for a pre-shock gas density  $10^{-9}$  g cm $^{-3}$ , chondrule-to-gas mass ratio of 3.75% and shock speed 8 km s $^{-1}$ . The disk gas is presumed to be cold enough to condense S, because at the time of chondrule formation, 2 Myr after CAI formation, the disk is in the passively heated protoplanetary disk stage (Chiang & Goldreich 1997). As the shock advances, radiation from already heated chondrules escapes to the pre-shock region, pre-heating chondrules (perhaps forming melt that draws fluffy aggregates into compact spheres before the shock hits). Peak temperatures are reached immediately after the shock hits and are  $\approx 2000$  K for these parameters. Peak temperatures are attributable to the combination of absorption of other chondrules’ radiation, thermal exchange with the compressed, heated gas, and the drag heating as the chondrules equilibrated to the gas velocity. This drag heating disappears in one aerodynamic stopping time, about 1 minute, implying initial cooling rates  $\sim 10^4$  K hr $^{-1}$ . Chondrules then cool from about 1700 K at the rates at which they pass many optical depths from the shock front,  $\sim 10 - 10^2$  K hr $^{-1}$  depending on the density of chondrules which provide the opacity (dust is predicted to evaporate in the shock: Morris & Desch 2010). The shock model predicts the cooling rate through the crystallization temperatures is proportional to the chondrule density. The two stages of cooling and the cooling rate proportional to chondrule density are robust predictions unique to the shock model.

These are to be compared to the thermal histories of chondrules in the X wind model, superimposed on Figure 1. Parameters for the “revealed stage”, in which  $\dot{M} = 1 \times 10^{-7} M_{\odot}$  yr $^{-1}$ , were adopted. Temperatures in the X wind model are too high initially to condense S (at least in a near-solar composition gas), do not heat by more than a few hundred K, do not reach temperatures several hundred K above the liquidus, and do not exhibit two stages of

cooling with fast initial cooling rate and slower cooling rate at lower temperatures. The chondrules’ cooling rates also are not proportional to the chondrule density.

To summarize, the shock model conforms to many constraints that the X wind model does not. It predicts thermal histories with cold initial temperature, rapid rise to the correct peak temperatures, rapid cooling at first, then slow cooling through the crystallization range. The X wind model predicts high initial temperatures, a limited temperature increase to the peak temperature, and a single cooling rate from the peak temperature. The shock model predicts that chondrule cooling rates, which determine textures, are proportional to the chondrule density, explaining why barred olivine textures, which demand fast cooling rates and therefore chondrule densities, are more prevalent in compound chondrules. The X wind model predicts no correlation of cooling rate with chondrule density, and no correlation of chondrule texture with compound chondrule frequency. The shock model is consistent with formation in the disk and therefore both the presence of condensate grains and chondrule-matrix chemical complementarity. The X wind model would predict no correlation between chondrules and the matrix in which they are sited, and explicitly predicts that matrix grains have never been heated. Either of the proposed mechanisms for shocks, gravitational instability and planetesimal bow shocks, is compatible with a 2 Myr delay between CAI and chondrule formation. The X wind model predicts contemporaneous production of CAIs and chondrules. The shock model makes detailed predictions about the chondrule formation environment and the thermal histories of chondrules; the X wind model is less detailed, but where it makes predictions these often fail to conform to constraints. The data overwhelmingly support an origin for chondrules in the disk, melted by nebular shocks, rather than formation in the X-wind environment.

## 6.2. CAI formation

The formation of CAIs is a major unsolved problem in meteoritics. Fluffy Type A CAIs and the precursors of other, melted, CAIs contain refractory minerals that condense at high temperatures (Grossman 2002; MacPherson 2003). Barometers of oxygen fugacity constrain this gas to be as reducing as one of solar composition. These factors point to condensation in the solar nebula, at a stage when it was very hot, implying formation at an early time and/or location closer to the Sun. At temperatures  $\approx 1500 - 1650$  K, for example, hibonites and other Ca,Al-rich minerals in CAIs would condense, but ferromagnesian silicates would not (Lodders 2003). Models of the structure of protoplanetary disks that include realistic opacity, convection and viscous heating predict temperatures  $> 1400$  K only inside about 0.5 AU, even if the mass accretion rate through the disk is as high as  $\dot{M} = 10^{-7} M_{\odot} \text{ yr}^{-1}$ , a



stage that can only last for  $\sim 0.5$  Myr or less. Formation of CAIs during this restricted time of the disk’s evolution is consistent with the inferred spread in CAI ages  $\approx 0.4$  Myr, derived from Al-Mg systematics (MacPherson et al. 1995; Kita et al. 2005, 2010; Shahar & Young 2007).

The main objection to this straightforward interpretation is the so-called “CAI storage problem”, the perceived inability of solids to remain in the protoplanetary disk for the  $\sim 2$  Myr needed so that CAIs can join chondrules in chondrites. Aerodynamic drag, in particular, is expected to cause CAIs to spiral in toward the Sun on timescales  $\sim 10^5$  yr (Weidenschilling 1977b). Cuzzi et al. (2003) have shown, however, that while the majority of CAIs may migrate inward on  $10^5 - 10^6$  yr timescales, turbulence causes CAIs to diffuse outward as well on the same timescales. This model predicts that smaller CAIs should diffuse outward more effectively than larger particles, explaining the greater prevalence of Type A CAIs relative to the larger Type B CAIs. Within the context of the same model, Cuzzi et al. (2005a, 2005b) have also shown that CAIs experience high temperatures for the long ( $\sim 10^4 - 10^5$  yr timescales needed for elements to diffuse across the so-called Wark-Lovering rims observed around many CAIs. The igneous textures of most CAIs are potentially explained by passage through nebular shocks, in much the same manner as chondrules are presumably melted. The peak temperatures and cooling rates are consistent with this scenario. It is not clear whether shocks that melted CAIs would have been identical to the ones that melted chondrules, or perhaps were just due to the same mechanism but acting in a different environment. It is also not clear that such shocks could have acted at the times needed to melt CAIs. In principle, however, shocks acting in the disk over many Myr could explain the igneous textures of most CAIs. Thus, storage of CAIs in the disk is not only allowed by disk models, but may be necessary to explain their mineralogy and textures.

The scenario outlined above is consistent with the mineralogy of CAIs, especially formation of CAIs in a reducing gas. In contrast, The X-wind model predicts that CAIs should condense in their own rock vapor, devoid of almost all  $H_2$  gas, and is not consistent at all with the low oxygen fugacity recorded by CAIs during their formation. The scenario outlined above also is consistent with an early formation of CAIs over a short interval, whereas the X wind model predicts that CAIs should form continuously over many Myr.

### 6.3. Short-lived Radionuclides

#### 6.3.1. Iron 60 and Others

Essentially the only explanation for the presence of  $^{60}\text{Fe}$  in the early solar system is that it was injected into the solar nebula by one nearby supernova, or a small number of nearby supernovae (Goswami et al. 2005; Meyer & Zinner 2006; Wadhwa et al. 2007). Irradiation within the solar nebula or in the X-wind environment fails to produce the observed initial abundance of this neutron-rich isotope, by many orders of magnitude (Leya et al. 2003; Gounelle 2006). An external stellar nucleosynthetic source is demanded. An AGB star has been suggested as the source (Wasserburg et al. 1994, 1995, 1996, 1998), but isotopic evidence argues against an AGB star origin (Wadhwa et al. 2007), as well as the fact that a nearby AGB star at the time and place of the solar system’s formation is exceedingly improbable (Kastner & Myers 1994; Ouellette et al. 2009). The only plausible stellar source is a core-collapse supernova, because massive stars ( $> 20 M_{\odot}$ ) can evolve off the main sequence and explode as supernovae in  $< 10$  Myr, before they disperse from their birth clusters. It is currently debated whether the solar nebula’s  $^{60}\text{Fe}$  originated in a single supernova, less than 1 pc away, or in many supernovae several parsecs distant. Constraining which scenario applies is important for determine what radionuclides are injected along with  $^{60}\text{Fe}$ . For a single supernova, the distances must be nearby, less than several parsecs (Looney et al. 2006). Injection by a single supernova, into the Sun’s protoplanetary disk (Chevalier 2000), has been advocated by Ouellette et al. (2005, 2007, 2010), who show that sufficient  $^{60}\text{Fe}$  could be injected into an extant protoplanetary disk if it were a few  $\times 0.1$  pc from an isotropically exploding supernova, or up to a few parsecs away from a supernova as clumpy as the ejecta in the Cassiopeia A supernova remnant (see also Looney et al. 2006). Gounelle & Meibom (2008) and Gaidos et al. (2009) have argued that young ( $< 1$  Myr old) disks  $< 1$  pc from a supernova are rare, occurring with  $< 1\%$  probability; Ouellette et al. (2010) likewise calculate a low probability  $\sim 1\%$  for a disk at 2 pc to be struck by ejecta. Additionally, injection into the disk requires much of the ejecta to condense into dust grains before encountering the disk: simulations show  $< 1\%$  of the intercepted gas ejecta is injected into a disk (Ouellette et al. 2007). Injection of gas into a molecular cloud, instead of a disk, in principle can occur as far as a few parsecs (Looney et al. 2006; Gaidos et al. 2009), but here again the injection efficiency of gas ejecta is  $\sim 1\%$  (Boss et al. 2010). Recent models of supernova shock-triggered collapse by Boss & Keiser (2010) do exhibit shock fronts that are thinner and denser than those previously considered, and may allow for greater injection efficiencies. At this point, injection from a single supernova into either a protoplanetary disk or molecular cloud are viable models, although they might entail improbable circumstances.

Gounelle et al. (2009) have proposed that the gas from which the Sun formed was

contaminated by several dozen core-collapse supernovae, then swept up into a molecular cloud several Myr before the solar system formed. Their “Supernova Propagation and Cloud Enrichment” (SPACE) model invokes an astrophysical setting like the Scorpius-Centaurus star-forming region, in which massive stars have triggered collapse of nearby molecular clouds (either by winds or supernova shocks), triggering a new round of massive star formation and supernovae, (cf. Preibisch & Zinnecker 1999). In their model, Gounelle et al. (2009) computed an average value  $^{60}\text{Fe}/^{56}\text{Fe} \approx 3 \times 10^{-6}$  in a molecular cloud over a 10-20 Myr span, assuming a half-life of 1.5 Myr; updating the half-life to 2.3 Myr (Rugel et al. 2009) potentially could raise the  $^{60}\text{Fe}$  abundance by an order of magnitude, assuming the molecular cloud takes 10 Myr to form the Sun. A weakness of the model is that the supernova ejecta is assumed to mix into the swept-up material with 100% efficiency. Simulations of supernova ejecta interacting with protoplanetary disks (Ouellette et al. 2007) and molecular clouds (Boss et al. 2010) typically find mixing efficiencies  $\sim 1\%$ . Gounelle et al. (2009) argue for high mixing efficiencies on the basis of simulations of the thermal instability in interstellar shocks that do suggest high mixing ratios (Koyama & Inutsuka 2002; Audit & Hennebelle 2010). These latter simulations, it should be noted, involve shock speeds of only a few  $\times 10 \text{ km s}^{-1}$ , for which the post-shock temperature is  $< 10^4 \text{ K}$  and is consistent with a thermally unstable gas. The shock speeds associated with supernova ejecta less than a few parsecs from the explosion center are necessarily  $\sim 10^3 \text{ km s}^{-1}$ , and in these shocks the post-shock gas is too hot to cool effectively. We expect the mixing efficiency of supernova ejecta with swept-up gas to be closer to 1% than 100%, and consider the mixing efficiency to be an unresolved issue with the SPACE model.

Assuming the validity of either model, we can estimate the abundances of other radionuclides injected along with  $^{60}\text{Fe}$ , especially the shortest lived of the SLRs,  $^{41}\text{Ca}$ ,  $^{36}\text{Cl}$ ,  $^{26}\text{Al}$ ,  $^{10}\text{Be}$  and  $^{53}\text{Mn}$ . Neither model is capable of explaining  $^{10}\text{Be}$ , which is not created by stellar nucleosynthesis; the case of  $^{10}\text{Be}$  is considered separately below. As for the others, it has been demonstrated that a single supernova can inject the other radionuclides in the observed meteoritic proportions, provided the progenitor is  $> 20 M_{\odot}$  so that when it undergoes core collapse it may result in the “faint supernova” type in which the innermost layers fall back onto the core (Umeda & Nomoto 2002, 2005; Nomoto et al. 2006; Tominaga et al. 2007). Because essentially all of the  $^{53}\text{Mn}$  in a supernova is produced in the innermost  $3 M_{\odot}$  (Nomoto et al. 2006), fallback of ejecta reduces the  $^{53}\text{Mn}/^{26}\text{Al}$  ratio in the ejecta by orders of magnitude, resulting in the observed meteoritic proportions of  $^{41}\text{Ca}$ ,  $^{26}\text{Al}$ ,  $^{60}\text{Fe}$  and  $^{53}\text{Mn}$  in the ejecta, assuming a reasonable 1 Myr delay before isotopic closure (Takigawa et al. 2008). The abundance of  $^{36}\text{Cl}$  in the early solar system appears to be too high to be explained by injection from a single supernova (see discussion in Hsu et al. 2006). Injection of material from a single nearby supernova, either into the disk or into the Sun’s molecular cloud core,

can simultaneously explain the abundances of the other shortest-lived radionuclides  $^{41}\text{Ca}$ ,  $^{26}\text{Al}$ ,  $^{60}\text{Fe}$  and  $^{53}\text{Mn}$ , if the progenitor was a massive star experiencing fallback.

Within the context of the SPACE model, injection of  $^{60}\text{Fe}$  from multiple supernovae may yield the meteoritic  $^{26}\text{Al}/^{60}\text{Fe}$  ratio in the solar nebula, but cannot explain the abundances of  $^{41}\text{Ca}$  and  $^{53}\text{Mn}$ . The SPACE model does not lead to significant quantities of SLRs with half-lives  $< 1$  Myr, because of the long timescales (10-20 Myr) associated with the formation of the molecular cloud, so  $^{41}\text{Ca}$  and  $^{36}\text{Cl}$  would be significantly underproduced. This underproduction is inconsistent with studies that indicate a correlation between  $^{26}\text{Al}$  and  $^{41}\text{Ca}$  (Sahijpal & Goswami 1998), unless  $^{26}\text{Al}$  is not derived primarily from these multiple supernovae. Likewise, the SPACE model unavoidably and significantly *overproduces*  $^{53}\text{Mn}$  (Gounelle et al. 2009). Models of supernova ejecta generally show a  $^{53}\text{Mn}/^{60}\text{Fe}$  ratio 10 - 100 times larger than the solar nebula ratio inferred from meteorites (Goswami & Vanhala 2000; Wadhwa et al. 2007; Sahijpal & Soni 2006). This general trend does not apply to ejecta from a single supernova, if the supernova’s progenitor was  $> 20 M_{\odot}$  and experienced fallback, but considering the average ejecta of dozens of supernovae of various masses, this outcome appears inevitable.

To summarize,  $^{60}\text{Fe}$  cannot be formed by the X-wind model and requires an external supernova source. The multiple supernovae in the SPACE model of Gounelle et al. (2009) explains the the abundance of  $^{60}\text{Fe}$  in the early solar system, assuming that mixing efficiencies approach unity. Production of  $^{41}\text{Ca}$ ,  $^{36}\text{Cl}$  and  $^{26}\text{Al}$  in the X-wind environment would not conflict with production of  $^{60}\text{Fe}$  in the SPACE model, but the SPACE model inevitably and significantly overproduces  $^{53}\text{Mn}$ , making it incompatible with the X-wind model for SLR production, which also contributes to  $^{53}\text{Mn}$ . Because of this severe overproduction of  $^{53}\text{Mn}$  relative to  $^{60}\text{Fe}$ , and because we expect mixing ratios of supernova ejecta should be  $\sim 1\%$ , we disfavor the SPACE model as the source of the solar system’s  $^{60}\text{Fe}$  and other SLRs. This suggests strongly that the source of the solar nebula’s  $^{60}\text{Fe}$  was instead a single core-collapse supernova with progenitor mass  $> 20 M_{\odot}$ , that experienced fallback onto the core. Such a supernova would have underproduced  $^{36}\text{Cl}$ , but could simultaneously explain the observed abundances of  $^{41}\text{Ca}$ ,  $^{26}\text{Al}$ ,  $^{60}\text{Fe}$  and  $^{53}\text{Mn}$  (Takigawa et al. 2008), without contributions from multiple supernovae of a previous generation of star formation. Because a single supernova is favored source for  $^{60}\text{Fe}$ , and because this scenario can explain all of the SLRs (except  $^{10}\text{Be}$ ) that the X-wind model produces, significant contributions of these SLRs from the X-wind most likely can be excluded.

### 6.3.2. *The Special Case of Beryllium 10*

Since evidence for  $^{10}\text{Be}$  in the solar nebula was discovered (McKeegan et al. 2000), it has been used to support the X-wind model. Because this SLR is not produced in supernovae, Gounelle et al. (2001) called it a potential “smoking gun” for the X-wind model. However, the data point to an origin for  $^{10}\text{Be}$  that is distinct from  $^{26}\text{Al}$  and the other SLRs. Marhas et al. (2002) analyzed a variety of meteoritic components thought to form early in the solar nebula, including a so-called FUN (fractionation and unknown nuclear effects) CAI, as well as hibonites. They found evidence for  $^{10}\text{Be}$  in samples with firm upper limits on initial  $^{26}\text{Al}$ , and concluded that  $^{10}\text{Be}$  was not correlated with  $^{26}\text{Al}$ , and the two SLRs were “decoupled,” having separate origins, a conclusion supported by subsequent studies (Ushikubo et al. 2006; Srinivasan et al. 2007). In addition, the initial abundances of  $^{10}\text{Be}$  in a variety of samples are remarkably uniform. Desch et al. (2004) reviewed the dozen or so measurements up to that date and found them to all cluster in a range  $^{10}\text{Be}/^9\text{Be} \approx 0.45 - 1.8 \times 10^{-3}$ . More measurements have been made since then, all of which again cluster in the same range (Marhas et al. 2002; MacPherson et al. 2003; Ushikubo et al. 2006; Chaussidon et al. 2006; Srinivasan et al. 2007; Liu et al. 2007). These data strongly suggest that the source of  $^{10}\text{Be}$  not only was distinct from the source of  $^{26}\text{Al}$  and other SLRs, but pre-dated the solar system.

Desch et al. (2004) interpret these data to mean that most of the  $^{10}\text{Be}$  was inherited from the interstellar medium, as  $^{10}\text{Be}$  GCRs that were slowed and trapped in the Sun’s molecular cloud core as it collapsed. They calculated the rate at which such low-energy ( $< 10 \text{ MeV nucleon}^{-1}$ ) GCRs were trapped in the Sun’s cloud core, accounting for magnetic focusing and mirroring, and computed an initial ratio in the solar system of  $^{10}\text{Be}/^9\text{Be} = 1.1 \times 10^{-3}$ . Other SLRs are not predicted to derive from this mechanism (Desch et al. 2004). To the extent that any fraction of the  $^{10}\text{Be}$  in the solar nebula comes from a source other than the X-wind, it exacerbates the problems of overproduction of  $^{10}\text{Be}$  in the X-wind, relative to other SLRs (§5.3). If Desch et al. (2004) are correct in their interpretation that nearly all the  $^{10}\text{Be}$  came from trapped GCRs, it effectively rules out the X-wind model for SLR production. Because of its important consequences for the X-wind model, the model of Desch et al. (2004) has been questioned; here we address these criticisms.

Desch et al. (2004) predicted that the  $^{10}\text{Be}/^9\text{Be}$  ratio was initially homogeneous within the solar nebula, as it represents material that was trapped in the molecular cloud core. In truth, fewer GCRs would reach and be stopped in the center of cloud core, so the  $^{10}\text{Be}/^9\text{Be}$  ratio would not have been completely homogeneous at this stage; it is difficult to judge the degree of heterogeneity at this stage, although it is probably less than a factor of 2. At any rate, it is presumed that such heterogeneities are erased as the cloud core continues to collapse into a protostar and disk, and the prediction of homogeneity of  $^{10}\text{Be}$  probably is

robust. Gounelle (2006) claimed that the variations in inferred initial  $^{10}\text{Be}/^9\text{Be}$  ratios point to a non-homogeneous distribution of  $^{10}\text{Be}$ . Likewise, Liu et al. (2007) analyzed platy hibonites from CM chondrites and found one with an initial ratio  $^{10}\text{Be}/^9\text{Be} = 5.5 \pm 1.4 \times 10^{-4}$  which, they claimed, was statistically significantly lower than the average values. Because platy hibonites are believed to be older than other components, this lower value is not attributed to decay of  $^{10}\text{Be}$  over time, implying that  $^{10}\text{Be}$  was spatially heterogeneous. Notably, though, Ushikubo et al. (2006) also measured platy hibonites from the CM2 chondrite Murchison and the CO3 chondrite Kainsaz, and inferred higher initial values in similar samples,  $^{10}\text{Be}/^9\text{Be} = 1.8 \pm 0.4 \times 10^{-3}$ . We choose to interpret the range of inferred initial  $^{10}\text{Be}/^9\text{Be}$  ratios as clustering about a uniform value, within the experimental uncertainties. Clearly, further analyses will determine whether observed variations reflect true nebular heterogeneities or differences in experimental techniques.

Gounelle (2006) also criticized many assumptions and other aspects of the Desch et al. (2004) model. First, they disputed the long cloud core collapse time  $\sim 10$  Myr used in the main simulation of Desch et al. (2004), implying that since observed collapse times of molecular cloud cores are  $\approx 0.3 - 1.6$  Myr, (Lee & Myers 1999), that perhaps Desch et al. (2004) overestimated the  $^{10}\text{Be}$  by a factor  $\approx 10$ . In fact, it is clear from Figure 3 of Desch et al. (2004) that the  $^{10}\text{Be}/^9\text{Be}$  quickly saturates to values  $\sim 1 \times 10^{-3}$ , so longer collapse times do *not* lead to higher  $^{10}\text{Be}/^9\text{Be}$  ratios. In fact, Desch et al. (2004) explored the sensitivity of  $^{10}\text{Be}$  abundance to magnetic field strength and therefore collapse time (their Figure 4). They found  $^{10}\text{Be}/^9\text{Be} \approx 1 \times 10^{-3}$  even for parameters that lead to collapse times  $< 1$  Myr. Gounelle (2006) also criticized the assumption of Desch et al. (2004) that the GCR flux was a factor of 2 higher 4.6 Gyr ago than today, calling it “ad hoc”. In fact, as explained by Desch et al. (2004), the GCR flux scales with the supernova rate, which scales with the star formation rate, which is well known to be decreasing over Galactic history. The GCR flux was definitely higher in the past than today, by a factor roughly 1.5 – 2.5 higher than today (Desch et al. 2004). Gounelle (2006) also criticized the fact that the simulations of Desch & Mouschovias (2001) used by Desch et al. (2004) formed a  $1 M_{\odot}$  star from a  $45 M_{\odot}$  cloud. We point out that the observed star formation efficiency is similarly low (Ward-Thompson et al. 2007), and that the exact cloud structure is somewhat irrelevant:  $^{10}\text{Be}$  GCRs will be trapped in collapsing cores, as demonstrated by Desch et al. (2004), as they transition from low densities transparent to low-energy GCRs to high densities opaque to GCRs, passing through surface densities  $\sim 10^{-2} \text{ g cm}^{-2}$ . This is true regardless of the details of the larger structures, because they are largely transparent to such GCRs. Other objections raised by Gounelle (2006), e.g., relating to the importance of magnetic mirroring, are addressed directly by Desch et al. (2004) The objections of Gounelle (2006) are readily refuted, and we consider the model of Desch et al. (2004) to be valid.

Beryllium 10 is known to be decoupled from the other SLRs and to have a separate source. The uniformity of the inferred initial  $^{10}\text{Be}/^9\text{Be}$  ratios around a value  $\approx 1 \times 10^{-3}$  strongly suggests an origin before the formation of the protoplanetary disk. The model of Desch et al. (2004) predicts  $^{10}\text{Be}/^9\text{Be} \approx 1 \times 10^{-3}$  due to trapping of low-energy  $^{10}\text{Be}$  GCRs as the Sun’s molecular cloud core contracts and becomes opaque to such GCRs. To the extent that  $^{10}\text{Be}$  in the early solar system can be attributed to trapped GCRs, then the contributions to  $^{10}\text{Be}$  must be significantly reduced or even excluded, effectively ruling out significant contributions to the SLRs from the X-wind.

## 7. Conclusions

The X-wind model was originally developed to explain the dynamics of bipolar outflows from protostars (Shu et al. 1994a,b, 1995; Najita & Shu 1994; Ostriker & Shu 1995). It remains a viable model for protostellar jets, although not the only one: “disk wind” models, in which the magnetocentrifugal outflows are launched from 0.1 - 1 AU, rather than from  $< 0.1$  AU, also exist (Wardle & Königl 1993; Königl & Pudritz 2000; Pudritz et al. 2007). Observational evidence from the rotation of protostellar jets tends to favor disk wind models (Bacciotti et al. 2002; Anderson 2003; Coffey et al. 2004, 2007; Woitas et al. 2005), and at this time the evidence for X-wind models in particular is not conclusive.

In a series of papers (Shu et al. 1996, 1997, 2001; Gounelle et al. 2001), the X-wind model was applied to three fundamental problems in meteoritics: the formation of chondrules, the formation of CAIs, and the origin of the SLRs. Progress toward an *astrophysical* theory of chondrites was sought. In this paper, we have shown that the X-wind model is not applicable to the formation of chondrules, to the formation of CAIs, nor the origin of the SLRs. We have demonstrated that the model itself has internal inconsistencies. It also makes predictions about chondrule and CAI formation at odds with experimental constraints. In regard to the SLRs, it does not satisfactorily explain the coproduction of  $^{10}\text{Be}$ ,  $^{26}\text{Al}$ ,  $^{41}\text{Ca}$  and  $^{53}\text{Mn}$ , and it leaves unexplained the source of  $^{60}\text{Fe}$  and  $^{36}\text{Cl}$ .

The internal inconsistencies can be summarized as follows. First, material is brought to the reconnection ring only because of accretion, yet the heating caused by this accretion was neglected in the X-wind model. When it is included, the model predicts temperatures too high for most silicate material to exist. This is consistent with astronomical observations, which also show no evidence for solids at the X point. Second, the X-wind model assumes rather arbitrarily that a fraction  $F \sim 0.01$  of all solid material falls out of the funnel flow and into the reconnection ring. This factor is not determined from first principles, and our own calculations presented here show that essentially all solids brought in from the disk will

remain entrained in the funnel flow and accreted on the star. Third, the X-wind model asserts that particles falling from the funnel flow will join a geometrically thin “reconnection ring”. In fact, particles leaving the funnel flow are likely to enter the reconnection ring with velocities comparable to the Keplerian orbital velocity there,  $> 100 \text{ km s}^{-1}$ , with significant orbital inclinations. It is not clear how these inclinations would be damped so particles could join the reconnection ring. Also, particles already in the reconnection ring would experience shattering collisions with incoming particles, at a rate sufficient to prevent particle growth in the reconnection ring. Fourth, the X-wind model neglects thermal sputtering by the plasma in the reconnection ring. We have shown that thermal sputtering will prevent growth of particles in the reconnection ring. Fifth, the X-wind model necessarily posits that CAIs and chondrules, formed in the reconnection ring, lie very close to the disk midplane ( $< 3 \times 10^9 \text{ cm}$ ), yet particles must be far from the midplane ( $> 4 \times 10^{10} \text{ cm}$ ) to be launched in a magnetocentrifugal outflow. Vertical diffusion of particles is not modeled. The MRI is invoked, but the magnetic diffusivity needed to allow gas to diffuse across the X point is close to the limit at which the MRI is suppressed. Sixth, the trajectories of particles launched in the magnetocentrifugal outflow are not explicitly modeled. It does seem clear, though, that the mechanism is extremely sensitive to the size of the particles, implying that only a small fraction of the material could be launched.

Ignoring these internal inconsistencies, the X-wind model makes a number of predictions about chondrules that are inconsistent with constraints on their origins. The thermal histories of chondrules are experimentally constrained by measurements of elemental and isotopic fractionation, and by chemical zoning and textures. The X-wind model does not allow chondrules to form from material containing primary S, as the starting temperatures are too high. It does not explain the very high peak temperatures of chondrules, nor the rapid cooling from the peak. It also predicts that all CAIs and chondrules melted in the X-wind will cool at  $10 \text{ K hr}^{-1}$ , which is not consistent with the cooling rates of barred olivine and some other chondrules,  $\sim 10^3 \text{ K hr}^{-1}$ . The observed correlation between compound chondrule frequency and textural type is also not predicted by the X-wind model. Very importantly, the X-wind model predicts that within a chondrite the chondrules are formed at  $< 0.1 \text{ AU}$  and the matrix grains at  $\approx 2 - 3 \text{ AU}$ , and that there should be no correlation between their compositions. This directly contradicts the observed chondrule-matrix chemical complementarity. Finally, the X-wind model predicts contemporaneous formation of chondrules and CAIs, which is contradicted by Pb-Pb dating and Al-Mg systematics, which show a 2 Myr age difference.

The X-wind model also makes a number of predictions about CAI formation. The assumption of a refractory Ca,Al-rich core surrounded by a ferromagnesian silicate mantle (necessary to prevent substantial overproduction of  $^{41}\text{Ca}$ ) is not supported by observed behaviors of CAI melts. Also, because CAIs are explicitly assumed to grow due to vapor



recondensation, the oxygen fugacity of the X-wind environment will be that of rock vapor itself; hydrogen and other volatile phases would be accreted by the funnel flow onto the star. This oxygen fugacity is orders of magnitude too oxidizing to be consistent with oxygen barometers of CAI formation, which routinely indicate a gas of solar composition. The discovery of osbornite in the CAI-like *Stardust* sample *Inti*, and in CAIs of Isheyev, likewise strongly indicate a gas of solar composition for the formation environments of these particular inclusions, and not an X-wind environment.

The X-wind model also makes a number of predictions about the production of SLRs. In the context of the X-wind model, even for the most favorable parameters (Gounelle et al. 2001),  $^{10}\text{Be}$  is overproduced, given that the cross section  $^{24}\text{Mg}(^3\text{He}, p)^{26}\text{Al}$  is measured to be 3 times smaller than Gounelle et al. (2001) assumed (Fitoussi et al. 2004). The overproduction of  $^{10}\text{Be}$  is more profound to the extent that  $^{10}\text{Be}$  has an external origin, such as trapped GCRs (Desch et al. 2004). In the context of the X-wind model, the only way to avoid severe overproduction of  $^{41}\text{Ca}$  is if almost all the Ca in the CAI were sequestered in a core, surrounded by a silicate mantle  $\sim 1$  cm thick. As Simon et al. (2002) point out, real CAI melts do not form immiscible liquids that would segregate in this way. Despite the likelihood that  $^{36}\text{Cl}$  in the solar nebula was created by irradiation, the X-wind environment is too hot for either the target nuclei or  $^{36}\text{Cl}$  to condense. Finally, the X-wind model cannot explain the existence of  $^{60}\text{Fe}$  in the solar nebula, because this neutron-rich isotope is not sufficiently produced by spallation.

The problems of the X-wind model are even starker in the face of the viable alternatives that exist in the literature. Chondrule formation is explained in great detail by melting in nebular shocks. This model is consistent with the detailed thermal histories of chondrules, their observed correlation with compound chondrule frequency, and chondrule-matrix complementarity. Formation of CAIs in the disk, during an earlier stage of disk evolution where the mass accretion rates were higher, is consistent with an earlier formation of CAIs than chondrules, with the solar oxygen fugacity of their formation environment, and allows some CAIs to remain unmelted. Finally, because  $^{60}\text{Fe}$  is not produced significantly in the X-wind environment, its source must be one or more nearby core-collapse supernovae. The overproduction of  $^{53}\text{Mn}$  relative to  $^{60}\text{Fe}$  appears to exclude multiple supernovae. Injection of material from a single, nearby core-collapse supernova is broadly consistent and can explain simultaneously the abundances of  $^{41}\text{Ca}$ ,  $^{26}\text{Al}$ ,  $^{60}\text{Fe}$  and  $^{53}\text{Mn}$  (Takigawa et al. 2008). Neither one nor several supernova, nor the X-wind model, appear capable of explaining the high inferred initial abundance of  $^{36}\text{Cl}$ , which may demand a separate origin in a late stage of irradiation in the early solar system. Supernova nucleosynthesis does not produce  $^{10}\text{Be}$ , but this SLR is known to be decoupled from  $^{26}\text{Al}$  and the other SLRs. A unique origin as trapped GCRs qualitatively and quantitatively explains its near-uniform abundance  $^{10}\text{Be}/^9\text{Be} \sim 10^{-3}$  in a

variety of meteoritic inclusions (Desch et al. 2004). Objections by Gounelle (2006) to the model of Desch et al. (2004) are readily refuted. The origins of the SLRs are still unknown and are the focus of ongoing research; but the working hypothesis of trapped  $^{10}\text{Be}$  GCRs and injection from a single supernova with fallback appears more viable than the X-wind model plus multiple supernovae for  $^{60}\text{Fe}$ . In short, viable and more plausible alternative models exist for all the meteoritic components the X-wind model purports to explain.

The X-wind model makes assumptions that are internally inconsistent. The X-wind model makes predictions about the formation of chondrules and CAIs and the production of SLRs that are contradicted by experimental constraints. Better alternative models exist to explain the formation of chondrules and CAIs and the production of SLRs. We conclude the X-wind model is irrelevant to the problems of chondrule formation, CAI formation, or the creation of short-lived radionuclides.

S. J. D. gratefully acknowledges the support for this work made available by NASA's Origins of Solar Systems Program, grant NNG06GI65G, and by the NASA Astrobiology Institute.

## REFERENCES

- Amelin, Y., Krot, A. N., Hutcheon, I. D., & Ulyanov, A. A. 2002, *Science*, 297, 1678
- Anderson, J. M., Li, Z.-Y., Krasnopolsky, R., & Blandford, R. D. 2003, *ApJ*, 590, L107
- Audit, E., & Hennebelle, P. 2010, *A&A*, 511, A76
- Bacciotti, F., Ray, T. P., Mundt, R., Eislöffel, J., & Solf, J. 2002, *ApJ*, 576, 222
- Beckett, J. R., Grossman, L., & Haggerty, S. E. 1986, *Meteoritics*, 21, 332
- Beckett, J. R., Simon, S. B., & Stolper, E. 2000, *Geochim. Cosmochim. Acta*, 64, 2519
- Beckett, J. R., Connolly, H. C., & Ebel, D. S. 2006, *Meteorites and the Early Solar System II*, 399
- Bizzarro, M., Baker, J. A., & Haack, H. 2004, *Nature*, 431, 275
- Blandford, R. D., & Payne, D. G. 1982, *MNRAS*, 199, 883
- Boley, A. C., & Durisen, R. H. 2008, *ApJ*, 685, 1193

- Boss, A. P., & Durisen, R. H. 2005, *ApJ*, 621, L137
- Boss, A. P., & Keiser, S. A. 2010, *ApJ*, 717, L1
- Boss, A. P., Keiser, S. A., Ipatov, S. I., Myhill, E. A., & Vanhala, H. A. T. 2010, *ApJ*, 708, 1268
- Bottke, W. F., Durda, D. D., Nesvorný, D., Jedicke, R., Morbidelli, A., Vokrouhlický, D., & Levison, H. F. 2005, *Icarus*, 179, 63
- Bouvier, A., & Wadhwa, M. 2009, *Lunar and Planetary Institute Science Conference Abstracts*, 40, 2184
- Cabrit, S., Pety, J., Pesenti, N., & Dougados, C. 2006, *A&A*, 452, 897
- Cameron, A. G. W., & Truran, J. W. 1977, *Icarus*, 30, 447
- Chaussidon, M., Robert, F., & McKeegan, K. D. 2006, *Geochim. Cosmochim. Acta*, 70, 224
- Chevalier, R. A. 2000, *ApJ*, 538, L151
- Chiang, E. I., & Goldreich, P. 1997, *ApJ*, 490, 368
- Ciesla, F. J. 2007, *Science*, 318, 613
- Ciesla, F. J., & Hood, L. L. 2002, *Icarus*, 158, 281
- Ciesla, F. J., & Hood, L. L. 2004, *Workshop on Chondrites and the Protoplanetary Disk*, 9057
- Ciesla, F. J. 2007, *Science*, 318, 613
- Coffey, D., Bacciotti, F., Woitas, J., Ray, T. P., & Eislöffel, J. 2004, *Ap&SS*, 292, 553
- Coffey, D., Bacciotti, F., Ray, T. P., Eislöffel, J., & Woitas, J. 2007, *ApJ*, 663, 350
- Connelly, J. N., Amelin, Y., Krot, A. N., & Bizzarro, M. 2008, *ApJ*, 675, L121
- Connolly, H. C., Jr., & Burnett, D. S. 2000, *Meteoritics and Planetary Science Supplement*, 35, 44
- Connolly, H. C., & Burnett, D. S. 2003, *Geochim. Cosmochim. Acta*, 67, 4429
- Connolly, H. C., Jr., & Desch, S. J. 2004, *Chemie der Erde / Geochemistry*, 64, 95
- Connolly, H. C., Jr., & Huss, G. R. 2010, *Geochim. Cosmochim. Acta*, 74, 2473

- Connolly, H. C., Jr., & Love, S. G. 1998, *Science*, 280, 62
- Connolly, H. C., Hewins, R. H., Ash, R. D., Zanda, B., Lofgren, G. E., & Bourot-Denise, M. 1994, *Nature*, 371, 136
- Connolly, H. C., Jr., Jones, B. D., & Hewins, R. H. 1998, *Geochim. Cosmochim. Acta*, 62, 2725
- Connolly, H. C., Jr., Burnett, D. S., & McKeegan, K. D. 2003, *Meteoritics and Planetary Science*, 38, 197
- Connolly, H. C., Jr., Desch, S. J., Ash, R. D., & Jones, R. H. 2006, *Meteorites and the Early Solar System II*, 383
- Connolly, H. C., et al. 2009, *Lunar and Planetary Institute Science Conference Abstracts*, 40, 1993
- Cuzzi, J. N., & Alexander, C. M. O. 2006, *Nature*, 441, 483
- Cuzzi, J. N., & Hogan, R. C. 2003, *Icarus*, 164, 127
- Cuzzi, J. N., Hogan, R. C., Paque, J. M., & Dobrovolskis, A. R. 2001, *ApJ*, 546, 496
- Cuzzi, J. N., Davis, S. S., & Dobrovolskis, A. R. 2003, *Icarus*, 166, 385
- Cuzzi, J. N., Petaev, M. I., Ciesla, F. J., Krot, A. N., & Scott, E. R. D. 2005a, 36th Annual Lunar and Planetary Science Conference, 36, 2095
- Cuzzi, J. N., Ciesla, F. J., Petaev, M. I., Krot, A. N., Scott, E. R. D., & Weidenschilling, S. J. 2005b, *Chondrites and the Protoplanetary Disk*, 341, 732
- Cuzzi, J. N., Hogan, R. C., & Shariff, K. 2008, *ApJ*, 687, 1432
- Davis, A. M., & MacPherson, G. J. 1996, *Chondrules and the Protoplanetary Disk*, 71
- Desch, S. J. 2004, *ApJ*, 608, 509
- Desch, S. J. 2007, *ApJ*, 671, 878
- Desch, S. J., & Connolly, H. C., Jr. 2002, *Meteoritics and Planetary Science*, 37, 183
- Desch, S. J., & Cuzzi, J. N. 2000, *Icarus*, 143, 87
- Desch, S. J., & Mouschovias, T. C. 2001, *ApJ*, 550, 314

- Desch, S. J., & Ouellette, N. 2006, *Geochim. Cosmochim. Acta*, 70, 5426
- Desch, S. J., Connolly, H. C., Jr., & Srinivasan, G. 2004, *ApJ*, 602, 528
- Desch, S. J., Ciesla, F. J., Hood, L. L., & Nakamoto, T. 2005, *Chondrites and the Protoplanetary Disk*, 341, 849
- Dodd, R. T., & van Schmus, W. R. 1971, *Chemie die Erde*, 30, 49
- Dominik, C., & Tielens, A. G. G. M. 1997, *ApJ*, 480, 647
- Draine, B. T., & Salpeter, E. E. 1979, *ApJ*, 231, 438
- Ebel, D. S. 2006, *Meteorites and the Early Solar System II*, 253
- Ebel, D. S., & Grossman, L. 2000, *Geochim. Cosmochim. Acta*, 64, 339
- Ebel, D. S., Weisberg, M. K., Hertz, J., & Campbell, A. J. 2008, *Meteoritics and Planetary Science*, 43, 1725
- Eisner, J. A., Hillenbrand, L. A., White, R. J., Akeson, R. L., & Sargent, A. I. 2005, *ApJ*, 623, 952
- Fedkin, A. V., Grossman, L., & Ghiorso, M. S. 2006, *37th Annual Lunar and Planetary Science Conference*, 37, 2249
- Fedkin, A. V., Ciesla, F. J., & Grossman, L. 2008, *Lunar and Planetary Institute Science Conference Abstracts*, 39, 1834
- Feigelson, E. D., & Montmerle, T. 1999, *ARA&A*, 37, 363
- Feigelson, E., Townsley, L., Güdel, M., & Stassun, K. 2007, *Protostars and Planets V*, 313
- Fitoussi, C., et al. 2004, *Lunar and Planetary Institute Science Conference Abstracts*, 35, 1586
- Gaidos, E., Krot, A. N., Williams, J. P., & Raymond, S. N. 2009, *ApJ*, 696, 1854
- Galy, A., Young, E. D., Ash, R. D., & O’Nions, R. K. 2000, *Science*, 290, 1751
- Getman, K. V., Feigelson, E. D., Broos, P. S., Micela, G., & Garmire, G. P. 2008, *ApJ*, 688, 418
- Ghosh, P., & Lamb, F. K. 1979, *ApJ*, 232, 259

- Gooding, J. L., & Keil, K. 1981, *Meteoritics*, 16, 17
- Gombosi, T. I., Nagy, A. F., & Cravens, T. E. 1986, *Reviews of Geophysics*, 24, 667
- Goswami, J. N., & Vanhala, H. A. T. 2000, *Protostars and Planets IV*, 963
- Goswami, J. N., Marhas, K. K., Chaussidon, M., Gounelle, M., & Meyer, B. S. 2005, *Chondrites and the Protoplanetary Disk*, 341, 485
- Gounelle, M. 2006, *New Astronomy Review*, 50, 596
- Gounelle, M., & Meibom, A. 2008, *ApJ*, 680, 781
- Gounelle, M., Shu, F. H., Shang, H., Glassgold, A. E., Rehm, K. E., & Lee, T. 2001, *ApJ*, 548, 1051
- Gounelle, M., Meibom, A., Hennebelle, P., & Inutsuka, S.-i. 2009, *ApJ*, 694, L1
- Grossman, J. N. 1988, *Meteorites and the Early Solar System*, 680
- Grossman, L. 1972, *Geochim. Cosmochim. Acta*, 36, 597
- Grossman, L. 2002, *Meteoritics and Planetary Science Supplement*, 37, 57
- Harker, D. E., & Desch, S. J. 2002, *ApJ*, 565, L109
- Hewins, R. H. 1997, *Annual Review of Earth and Planetary Sciences*, 25, 61
- Hewins, R. H., & Connolly, H. C., Jr. 1996, *Chondrules and the Protoplanetary Disk*, 197
- Hewins, R., Jones, R., & Scott, E. 1996, *Chondrules and the Protoplanetary Disk*, Edited by Roger Hewins and Rhian Jones and Ed Scott, pp. 360. ISBN 0521552885. Cambridge, UK: Cambridge University Press, June 1996.
- Hewins, R. H., Connolly, H. C., Lofgren, G. E., Jr., & Libourel, G. 2005, *Chondrites and the Protoplanetary Disk*, 341, 286
- Hezel, D. C., & Palme, H. 2008, *Earth and Planetary Science Letters*, 265, 716
- Hogan, R. C., & Cuzzi, J. N. 2007, *Physical Review E*, 75, 056305
- Hood, L. L., *Metic. Plan. Sci.* 33, 97
- Hood, L. L., & Horanyi, M. 1991, *Icarus* 93, 259
- Hood, L. L., & Horanyi, M. 1993, *Icarus* 106, 179

- Hood, L. L., Ciesla, F. J., Artemieva, N. A., Marzari, F., & Weidenschilling, S. J. 2009, *Meteoritics and Planetary Science*, 44, 327
- Hsu, W., Guan, Y., Leshin, L. A., Ushikubo, T., & Wasserburg, G. J. 2006, 37th Annual Lunar and Planetary Science Conference, 37, 2028
- Hubeny, I. 1990, *ApJ*, 351, 632
- Huss, G. R., & Meyer, B. S. 2009, Lunar and Planetary Institute Science Conference Abstracts, 40, 1957
- Huss, G. R., MacPherson, G. J., Wasserburg, G. J., Russell, S. S., & Srinivasan, G. 2001, *Meteoritics and Planetary Science*, 36, 975
- Hutcheon, I. D., Marhas, K. K., Krot, A. N., Goswami, J. N., & Jones, R. H. 2009, *Geochim. Cosmochim. Acta*, 73, 5080
- Iida, A., Nakamoto, T., Susa, H., & Nakagawa, Y. 2001, *Icarus*, 153, 430
- Jacobsen, S. B. 2005, *Chondrites and the Protoplanetary Disk*, 341, 548
- Jacobsen, B., Matzel, J., Hutcheon, I. D., Ramon, E., Krot, A. N., Ishii, H. A., Nagashima, K., & Yin, Q.-Z. 2009, *Geochimica et Cosmochimica Acta Supplement*, 73, 580
- Jones, A. P. 2004, *Astrophysics of Dust*, 309, 347
- Jones, R. H. 1996, *Chondrules and the Protoplanetary Disk*, 163
- Jones, R. H., & Lofgren, G. E. 1993, *Meteoritics*, 28, 213
- Jones, R. H., Lee, T., Connolly, H. C., Jr., Love, S. G., & Shang, H. 2000, *Protostars and Planets IV*, 927
- Kama, M., Min, M., & Dominik, C. 2009, *A&A*, 506, 1199
- Kastner, J. H., & Myers, P. C. 1994, *ApJ*, 421, 605
- Kita, N. T., Huss, G. R., Tachibana, S., Amelin, Y., Nyquist, L. E., & Hutcheon, I. D. 2005, *Chondrites and the Protoplanetary Disk*, 341, 558
- Kita, N. T., Kimura, M., Ushikubo, T., Valley, J. W., & Nyquist, L. E. 2008, Lunar and Planetary Institute Science Conference Abstracts, 39, 2059

- Kita, N. T., Ushikubo, T., Davis, A. M., Knight, K. B., Mendybaev, R. A., Richter, F. M., & Fournelle, J. H. 2010, Lunar and Planetary Institute Science Conference Abstracts, 41, 2154
- Klerner, S., & Palme, H. 2000, Meteoritics and Planetary Science Supplement, 35, 89
- Konigl, A., & Pudritz, R. E. 2000, Protostars and Planets IV, 759
- Koyama, H., & Inutsuka, S.-i. 2002, ApJ, 564, L97
- Krot, A. N., Fegley, B., Jr., Lodders, K., & Palme, H. 2000, Protostars and Planets IV, 1019
- Larimer, J. W. 1967, Geochim. Cosmochim. Acta, 31, 1215
- Lauretta, D. S., Buseck, P. R., & Zega, T. J. 2001, Geochim. Cosmochim. Acta, 65, 1337
- Lauretta, D. S., Nagahara, H., & Alexander, C. M. O. 2006, Meteorites and the Early Solar System II, 431
- Lee, C.-F., Ho, P. T. P., Beuther, H., Bourke, T. L., Zhang, Q., Hirano, N., & Shang, H. 2006, ApJ, 639, 292
- Lee, C.-F., Ho, P. T. P., Hirano, N., Beuther, H., Bourke, T. L., Shang, H., & Zhang, Q. 2007, ApJ, 659, 499
- Lee, C. W., & Myers, P. C. 1999, ApJS, 123, 233
- Lee, T., Papanastassiou, D. A., & Wasserburg, G. J. 1976, Geophys. Res. Lett., 3, 41
- Lee, T., Shu, F. H., Shang, H., Glassgold, A. E., & Rehm, K. E. 1998, ApJ, 506, 898
- Levy, E. H. 1988, Meteorites and the Early Solar System, 697
- Leya, I., Halliday, A. N., & Wieler, R. 2003, ApJ, 594, 605
- Liffman, K., & Brown, M. 1995, Icarus, 116, 275
- Liffman, K., & Brown, M. J. I. 1996, Chondrules and the Protoplanetary Disk, pages 285-302, 285
- Lin, Y., Guan, Y., Leshin, L. A., Ouyang, Z., & Wang, D. 2005, Proceedings of the National Academy of Sciences 102: 1306-1311
- Liu, M.-C., McKeegan, K. D., Davis, A. M., & Ireland, T. R. 2007, Chronology of Meteorites and the Early Solar System, 102



- Lodders, K. 2003, *ApJ*, 591, 1220
- Lofgren, G. E. 1996, *Chondrules and the Protoplanetary Disk*, 187
- Lofgren, G., & Russell, W. J. 1986, *Geochim. Cosmochim. Acta*, 50, 1715
- Lofgren, G., & Lanier, A. B. 1990, *Geochim. Cosmochim. Acta*, 54, 3537
- Looney, L. W., Tobin, J. J., & Fields, B. D. 2006, *ApJ*, 652, 1755
- Lugmair, G. W., & Shukolyukov, A. 2001, *Meteoritics and Planetary Science*, 36, 1017
- MacPherson, G. J. 2003, *Treatise on Geochemistry*, Vol. 1, Meteorites, Comets and Planets (A. M. Davis, ed.), pp. 1-47.
- MacPherson, G. J., Grossman, L., Hashimoto, A., Bar-Matthews, M., & Tanaka, T. 1984, *J. Geophys. Res.*, 89, 299
- MacPherson, G. J., Davis, A. M., & Zinner, E. K. 1995, *Meteoritics*, 30, 365
- MacPherson, G. J., Huss, G. R., & Davis, A. M. 2003, *Geochim. Cosmochim. Acta*, 67, 3165
- MacPherson, G. J., Kita, N. T., Ushikubo, T., Bullock, E. S., & Davis, A. M. 2010, *Lunar and Planetary Institute Science Conference Abstracts*, 41, 2356
- Marhas, K. K., Goswami, J. N., & Davis, A. M. 2002, *Science*, 298, 2182
- McKeegan, K. D., Chaussidon, M., & Robert, F. 2000, *Science*, 289, 1334
- McKeegan, K. D., & Davis, A. M. 2003, *Treatise on Geochemistry*, 1, 431
- Meibom, A., Krot, A. N., Robert, F., Mostefaoui, S., Russell, S. S., Petaev, M. I., & Gounelle, M. 2007, *ApJ*, 656, L33
- Merrill, G. P. 1920, *Proceedings of the National Academy of Science*, 6, 449
- Meyer, B. S., & Huss, G. R. 2009, *Lunar and Planetary Institute Science Conference Abstracts*, 40, 1756
- Miura, H., & Nakamoto, T. 2006, *ApJ*, 651, 1272
- Morris, M. A., & Desch, S. J. 2010, *ApJ*, in press
- Murty, S. V. S., Goswami, J. N., & Shukolyukov, Y. A. 1997, *ApJ*, 475, L65
- Najita, J. R., & Shu, F. H. 1994, *ApJ*, 429, 808

- Nomoto, K., Tominaga, N., Umeda, H., Kobayashi, C., & Maeda, K. 2006, *Nuclear Physics A*, 777, 424
- Ostriker, E. C., & Shu, F. H. 1995, *ApJ*, 447, 813
- Ouellette, N., Desch, S. J., Hester, J. J., & Leshin, L. A. 2005, *Chondrites and the Protoplanetary Disk*, 341, 527
- Ouellette, N., Desch, S. J., & Hester, J. J. 2007, *ApJ*, 662, 1268
- Ouellette, N., Desch, S. J., Bizzarro, M., Boss, A. P., Ciesla, F., & Meyer, B. 2009, *Geochim. Cosmochim. Acta*, 73, 4946
- Ouellette, N., Desch, S. J., & Hester, J. J. 2010, *ApJ*, 711, 597
- Palme, H., Spettel, B., & Ikeda, Y. 1993, *Meteoritics*, 28, 417
- Paque, J. M., & Stolper, E. 1983, *Lunar and Planetary Institute Science Conference Abstracts*, 14, 596
- Paque, J. M., Sutton, S. R., Burnett, D. S., Beckett, J. R., & Simon, S. B. 2010, *Lunar and Planetary Institute Science Conference Abstracts*, 41, 1391
- Petaev, M. I., Meibom, A., Krot, A. N., Wood, J. A., & Keil, K. 2001, *Meteoritics and Planetary Science*, 36, 93
- Pety, J., Gueth, F., Guilloteau, S., & Dutrey, A. 2006, *A&A*, 458, 841
- Pilipp, W., Hartquist, T. W., Morfill, G. E., & Levy, E. H. 1998, *A&A*, 331, 121
- Preibisch, T., & Zinnecker, H. 1999, *AJ*, 117, 2381
- Pudritz, R. E., Ouyed, R., Fendt, C., & Brandenburg, A. 2007, *Protostars and Planets V*, 277
- Radomsky, P. M., & Hewins, R. H. 1990, *Geochim. Cosmochim. Acta*, 54, 3475
- Ray, T., Dougados, C., Bacciotti, F., Eisloffel, J., & Chrysostomou, A. 2007, *Protostars and Planets V*, 231
- Rubin, A. 1999, *Geochim. Cosmochim. Acta*, 63, 2281
- Rudraswami, N. G., Goswami, J. N., Chattopadhyay, B., Sengupta, S. K., & Thapliyal, A. P. 2008, *Earth and Planetary Science Letters*, 274, 93

- Rugel, G., et al. 2009, *Physical Review Letters*, 103, 072502
- Russell, S. S., Huss, G. R., MacPherson, G. J., & Wasserburg, G. J. 1997, *Lunar and Planetary Institute Conference Abstracts*, 28, 1209
- Russell, S. S., Hartmann, L., Cuzzi, J., Krot, A. N., Gounelle, M., & Weidenschilling, S. 2006, *Meteorites and the Early Solar System II*, 233
- Ruzicka, A., Floss, C., & Hutson, M. 2008, *Geochim. Cosmochim. Acta*, 72, 5530
- Sahijpal, S., & Goswami, J. N. 1998, *ApJ*, 509, L137
- Sahijpal, S., & Gupta, G. 2009, *Meteoritics and Planetary Science*, 44, 879
- Sahijpal, S., & Soni, P. 2006, *Meteoritics and Planetary Science*, 41, 953
- Sanders, I. S. 1996, *Chondrules and the Protoplanetary Disk*, 327
- Sargent, B. A., et al. 2009, *ApJS*, 182, 477
- Scott, E. R. D., & Krot, A. N. 2005, *ApJ*, 623, 571
- Shahar, A., & Young, E. D. 2007, *Earth and Planetary Science Letters*, 257, 497
- Shang, H., Shu, F. H., Lee, T., & Glassgold, A. E. 2000, *Space Science Reviews*, 92, 153
- Shu, F., Najita, J., Ostriker, E., Wilkin, F., Ruden, S., & Lizano, S. 1994a, *ApJ*, 429, 781
- Shu, F. H., Najita, J., Ruden, S. P., & Lizano, S. 1994b, *ApJ*, 429, 797
- Shu, F. H., Najita, J., Ostriker, E. C., & Shang, H. 1995, *ApJ*, 455, L155
- Shu, F. H., Shang, H., & Lee, T. 1996, *Science*, 271, 1545
- Shu, F. H., Shang, H., Glassgold, A. E., & Lee, T. 1997, *Science*, 277, 1475
- Shu, F. H., Najita, J. R., Shang, H., & Li, Z.-Y. 2000, *Protostars and Planets IV*, 789
- Shu, F. H., Shang, H., Gounelle, M., Glassgold, A. E., & Lee, T. 2001, *ApJ*, 548, 1029
- Simon, S. B., Davis, A. M., & Grossman, L. 1996, *Meteoritics and Planetary Science*, 31, 106
- Simon, S. B., Davis, A. M., Grossman, L., & McKeegan, K. D. 2002, *Meteoritics and Planetary Science*, 37, 533

- Simon, S. B., Sutton, S. R., & Grossman, L. 2010, Lunar and Planetary Institute Science Conference Abstracts, 41, 1459
- Skinner, S. L., & Walter, F. M. 1998, ApJ, 509, 761
- Sorby, H. C. 1877, Nature, 16, 23
- Srinivasan, G., Chaussidon, M., & Bischoff, A. 2007, Lunar and Planetary Institute Science Conference Abstracts, 38, 1781
- Stolper, E. 1982, Geochim. Cosmochim. Acta, 46, 2159
- Stolper, E., & Paque, J. M. 1986, Geochim. Cosmochim. Acta, 50, 1785
- Tachibana, S., & Huss, G. R. 2003, ApJ, 588, L41
- Tachibana, S., & Huss, G. R. 2005, Geochim. Cosmochim. Acta, 69, 3075
- Tachibana, S., Nagahara, H., Mostefaoui, S., & Kita, N. T. 2003, Meteoritics and Planetary Science, 38, 939
- Takigawa, A., Miki, J., Tachibana, S., Huss, G. R., Tominaga, N., Umeda, H., & Nomoto, K. 2008, ApJ, 688, 1382
- Teitler, S. A., Paque, J. M., Cuzzi, J. N., & Hogan, R. C. 2009, Lunar and Planetary Institute Science Conference Abstracts, 40, 2388
- Tominaga, N., Umeda, H., & Nomoto, K. 2007, ApJ, 660, 516
- Umeda, H., & Nomoto, K. 2002, ApJ, 565, 385
- Umeda, H., & Nomoto, K. 2005, ApJ, 619, 427
- Urey, H. C. 1967, Icarus, 7, 350
- Urey, H. C., & Craig, H. 1953, Geochim. Cosmochim. Acta, 4, 36
- Ushikubo, T., Guan, Y., & Leshin, L. A. 2006, 37th Annual Lunar and Planetary Science Conference, 37, 2368
- Vanhala, H. A. T., & Boss, A. P. 2002, ApJ, 575, 1144
- Villeneuve, J., Chaussidon, M., & Libourel, G. 2009, *Science* 325, 985
- Wadhwa, M., & Russell, S. S. 2000, Protostars and Planets IV, 995

- Wadhwa, M., Amelin, Y., Davis, A. M., Lugmair, G. W., Meyer, B., Gounelle, M., & Desch, S. J. 2007, *Protostars and Planets V*, 835
- Ward-Thompson, D., André, P., Crutcher, R., Johnstone, D., Onishi, T., & Wilson, C. 2007, *Protostars and Planets V*, 33
- Wardle, M., & Koenigl, A. 1993, *ApJ*, 410, 218
- Wasserburg, G. J., Busso, M., Gallino, R., & Raiteri, C. M. 1994, *ApJ*, 424, 412
- Wasserburg, G. J., Gallino, R., Busso, M., Goswami, J. N., & Raiteri, C. M. 1995, *ApJ*, 440, L101
- Wasserburg, G. J., Busso, M., & Gallino, R. 1996, *ApJ*, 466, L109
- Wasserburg, G. J., Gallino, R., & Busso, M. 1998, *ApJ*, 500, L189
- Wasson, J. T., Krot, A. N., Min, S. L., & Rubin, A. E. 1995, *Geochim. Cosmochim. Acta*, 59, 1847
- Weidenschilling, S. J. 1977a, *Ap&SS*, 51, 153
- Weidenschilling, S. J. 1977b, *MNRAS*, 180, 57
- Weidenschilling, S. J., Davis, D. R., & Marzari, F. 2001, *Earth, Planets, and Space*, 53, 1093
- Weisberg, M. K., & Prinz, M. 1996, *Chondrites and the Protoplanetary Disk* (eds. R. H. Hewins, R. H. Jones & E. R. D. Scott), 119.
- Woitak, J., Bacciotti, F., Ray, T. P., Marconi, A., Coffey, D., & Eisloffel, J. 2005, *Å*
- Wood, J. A. 1963, *Sci. Am.* 209, 64
- Young, E. D., Simon, J. I., Galy, A., Russell, S. S., Tonui, E., & Lovera, O. 2005, *Science*, 308, 223
- Yu, Y., Hewins, R. H., & Eiben, B. A. 1995, *Meteoritics*, 30, 604
- Yu, Y., & Hewins, R. H. 1998, *Geochim. Cosmochim. Acta*, 62, 159
- Zanda, B., Bourot-Denise, M., Perron, C., & Hewins, R. H. 1994, *Science*, 265, 1846
- Zanda, B. 2004, *Earth and Planetary Science Letters*, 224, 1
- Zolensky, M. E., et al. 2006, *Science*, 314, 1735



Table 1. Short-lived radionuclides in the early solar system

Parent Isotope	$T_{1/2}^a$	Daughter Isotope	Solar System Initial Abundance
$^{41}\text{Ca}$	0.1	$^{41}\text{K}$	$^{41}\text{Ca}/^{40}\text{Ca} \approx 1.5 \times 10^{-8}$
$^{36}\text{Cl}$	0.3	$^{36}\text{Ar}(98.1\%)$ $^{36}\text{S}(1.9\%)$	$^{36}\text{Cl}/^{35}\text{Cl} \approx 1.6 \times 10^{-4} ?$
$^{26}\text{Al}$	0.72	$^{26}\text{Mg}$	$^{26}\text{Al}/^{27}\text{Al} \approx 5.7 \times 10^{-5}$
$^{60}\text{Fe}$	1.5	$^{60}\text{Ni}$	$^{60}\text{Fe}/^{56}\text{Fe} \approx 3\text{-}10 \times 10^{-7}$
$^{10}\text{Be}$	1.5	$^{10}\text{B}$	$^{10}\text{Be}/^9\text{Be} \approx 10^{-3}$
$^{53}\text{Mn}$	3.7	$^{53}\text{Cr}$	$^{53}\text{Mn}/^{55}\text{Mn} \approx 10^{-5}$
$^{107}\text{Pd}$	6.5	$^{107}\text{Ag}$	$^{107}\text{Pd}/^{108}\text{Pd} \approx 5\text{-}40 \times 10^{-5}$
$^{182}\text{Hf}$	8.9	$^{182}\text{W}$	$^{182}\text{Hf}/^{180}\text{Hf} \approx 10^{-4}$
$^{129}\text{I}$	15.7	$^{129}\text{Xe}$	$^{129}\text{I}/^{129}\text{Xe} \approx 10^{-4}$

<sup>a</sup>Half-life in millions of years.

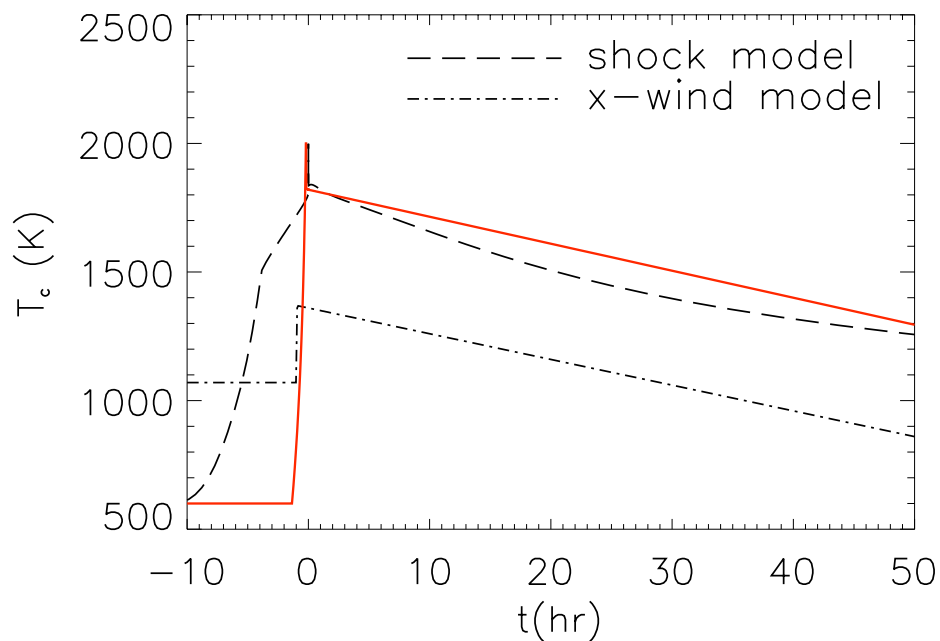


Fig. 1.— Chondrule thermal histories as inferred from experimental constraints (solid curve), as predicted by the shock model [from Morris & Desch (2010)] (dashed curve), and as predicted by the X-wind model during the “revealed stage” [adapted from Shu et al. (1996, 2001)] (dashed-dot curve). Chondrules in the X-wind model start too hot to condense S from a solar-composition gas, fail to reach the necessary peak temperatures, and show no rapid cooling from the peak that is needed to retain Na. Except for the prediction of an extended period of pre-shock heating, the shock model conforms well to all the constraints.